

## Trophic position increases with thermocline depth in yellowfin and bigeye tuna across the Western and Central Pacific Ocean



Patrick Houssard<sup>a,b</sup>, Anne Lorrain<sup>a,\*</sup>, Laura Tremblay-Boyer<sup>c</sup>, Valérie Allain<sup>c</sup>, Brittany S. Graham<sup>d</sup>, Christophe E. Menkes<sup>e</sup>, Heidi Pethybridge<sup>f</sup>, Lydie I.E. Couturier<sup>g</sup>, David Point<sup>h</sup>, Bruno Leroy<sup>c</sup>, Aurore Receveur<sup>c</sup>, Brian P.V. Hunt<sup>i,j</sup>, Elodie Vourey<sup>c</sup>, Sophie Bonnet<sup>k</sup>, Martine Rodier<sup>l</sup>, Patrick Raimbault<sup>m</sup>, Eric Feunteun<sup>n,o</sup>, Petra M. Kuhnert<sup>p</sup>, Jean-Marie Munaron<sup>g</sup>, Benoit Lebreton<sup>q</sup>, Tsuguo Otake<sup>r</sup>, Yves Letourneur<sup>b</sup>

<sup>a</sup> Institut de Recherche pour le Développement (IRD), LEMAR – UMR 6539 (UBO, CNRS, IRD, IFREMER), BP A5, 98848 Nouméa cedex, New Caledonia

<sup>b</sup> Université de la Nouvelle-Calédonie, LIVE – EA 4243, LabEx « Corail », BP R4, 98851 Nouméa cedex, New Caledonia

<sup>c</sup> Pacific Community, Oceanic Fisheries Programme, BP D5, 98848 Nouméa, New Caledonia

<sup>d</sup> National Institute of Water and Atmospheric Research (NIWA), Wellington, New Zealand

<sup>e</sup> IRD/Sorbonne Universités (UPMC, Université Paris 06)/CNRS/MNH, LOCEAN – UMR 7159, BP A5, 98848 Nouméa cedex, New Caledonia

<sup>f</sup> CSIRO Oceans and Atmosphere, GPO Box 1538, Hobart, TAS 2001, Australia

<sup>g</sup> Université de Brest, Laboratoire des Sciences de l'Environnement Marin (LEMAR, UMR 6539 IRD/UBO/CNRS/Ifremer), Institut Universitaire Européen de la Mer, 29280 Plouzané, France

<sup>h</sup> Observatoire Midi-Pyrénées, GET, UMR CNRS 5563/IRD 234/Université Paul Sabatier Toulouse 3, 14 avenue Edouard Belin, 31400 Toulouse, France

<sup>i</sup> Institute for the Oceans and Fisheries, University of British Columbia, Vancouver, V6T 1 Z4, British Columbia, Canada

<sup>j</sup> Hakai Institute, P.O. Box 309, Heriot Bay, BC V0P 1H0, Canada

<sup>k</sup> IRD, AMU/ CNRS/INSU, Université de Toulon, Mediterranean Institute of Oceanography (MIO) UM 110, 98848, Noumea, New Caledonia

<sup>l</sup> IRD/Université de la Polynésie Française/Institut Malmarmé/Ifremer, EIO – UMR 241 98700, Papeete, French Polynesia

<sup>m</sup> Aix Marseille Université, CNRS/INSU, Université de Toulon, IRD, Mediterranean Institute of Oceanography (MIO) UM 110, 13288 Marseille, France

<sup>n</sup> Muséum National d'Histoire Naturelle, UMR 7208 BOREA (Biologie Organismes Ecosystèmes Aquatiques) (MNHN, CNRS, UPMC, UniCaen, IRD, Univ Antilles), France

<sup>o</sup> Station Marine de Dinard-CRESCO, 38 Avenue du Port Blanc, 35800 Dinard, France

<sup>p</sup> CSIRO Data61, GPO Box 664, Canberra, ACT 2601, Australia

<sup>q</sup> UMR 7266 Littoral, Environnement et Sociétés (CNRS – Université de la Rochelle), Institut du littoral et de l'environnement, 17000 La Rochelle, France

<sup>r</sup> Department of Fishery Science, Faculty of Agricultural Life Science, 1-1-1 Yayoi, Bunkyo-ku, Tokyo 113-8657, Japan

### ARTICLE INFO

#### Article history:

Received 4 September 2016

Received in revised form 24 March 2017

Accepted 19 April 2017

Available online 21 April 2017

#### Keywords:

Nitrogen isotopes

POM

Isoscapes

Bigeye tuna

Yellowfin tuna

Depth of the 20°C isotherm

Amino acid

Compound-specific isotope analysis

Biochemical markers

### ABSTRACT

Estimates of trophic position are used to validate ecosystem models and understand food web structure. A consumer's trophic position can be estimated by the stable nitrogen isotope values ( $\delta^{15}\text{N}$ ) of its tissue, once the baseline isotopic variability has been accounted for. Our study established the first data-driven baseline  $\delta^{15}\text{N}$  isoscape for the Western and Central Pacific Ocean using particulate organic matter. Bulk  $\delta^{15}\text{N}$  analysis on 1039 muscle tissue of bigeye and yellowfin tuna were conducted together with amino acid compound-specific  $\delta^{15}\text{N}$  analysis (AA-CSIA) on a subset of 21 samples. Both particulate organic matter and tuna bulk  $\delta^{15}\text{N}$  values varied by more than 10‰ across the study area. Fine-scaled trophic position maps were constructed and revealed higher tuna trophic position (by  $\sim 1$ ) in the southern latitudes compared to the equator. AA-CSIA confirmed these spatial patterns for bigeye and, to a lesser extent, yellowfin tuna. Using generalized additive models, spatial variations of tuna trophic positions were mainly related to the depth of the 20°C isotherm, a proxy for the thermocline behavior, with higher tuna trophic position estimates at greater thermocline depths. We hypothesized that a deeper thermocline would increase tuna vertical habitat and access to mesopelagic prey of higher trophic position. Archival tagging data further suggested that the vertical habitat of bigeye tuna was deeper in the southern latitudes than at the equator. These results suggest the importance of thermocline depth in influencing tropical tuna diet, which affects their vulnerability to fisheries, and may be altered by climate change.

© 2017 Elsevier Ltd. All rights reserved.

\* Corresponding author.

E-mail address: [anne.lorrain@ird.fr](mailto:anne.lorrain@ird.fr) (A. Lorrain).

## 1. Introduction

Food web structure in oceanic environments can be altered by fishing at the top of the food web (Marasco et al., 2007; Baum and Worm, 2009; Estes et al., 2011) and by climate variability (Hays et al., 2005; Polovina et al., 2008). Long-term and progressive changes in food web structure have been shown to impact higher trophic levels, including commercially valuable tuna (Olson et al., 2014), and can affect the functioning, resilience and health of an ecosystem (e.g., productivity and services). Understanding the effects of fishing and climate on the trophic structure of marine exploited ecosystems is of worldwide interest to identify the most affected areas and species, and develop ecosystem-based management scenarios and strategies (Hobday et al., 2015; Young et al., 2015). Measures of trophic position in top predators can be used as a metric to describe aspects of food web and ecosystem structure, and detect changes at time scales relevant to management (year to decades).

In the tropical Pacific Ocean, tuna contribute significantly to the livelihoods, food and economic security of many island nations (Bell et al., 2015). Yellowfin tuna (*Thunnus albacares*) primarily occupy the epipelagic zone (Brill et al., 1999; Gunn and Block, 2001), hence exploiting prey resources near the surface (Schaefer et al., 2009) while bigeye tuna (*Thunnus obesus*) have physiological capabilities (Brill et al., 2005) that allow them to dive deeper and to exploit meso- and bathypelagic prey resources (Schaefer and Fuller, 2002; Young et al., 2010; Lam et al., 2014; Fuller et al., 2015). Despite apparent generalist feeding in tuna, previous studies have shown that differences in vertical feeding behavior, due to difference in thermocline depth, could explain inter- and intra-specific dietary differences over relatively short distances (Olson et al., 2010; Williams et al., 2015). The Western and Central Pacific Ocean is a highly dynamic oceanic region with strong latitudinal and longitudinal variations in mixed layer depth, thermocline depth, oxygen, nutrients and, in turn, phytoplankton communities (Longhurst, 2007; Le Borgne et al., 2011). These fundamental ecosystem properties largely determine the distribution of tuna species and could influence their feeding strategies (e.g., Ganachaud et al., 2013; Fuller et al., 2015). Knowledge of spatial variability in tuna foraging strategies across those regions is an important step to predicting how climate is likely to affect fish stocks and the viability of fishing industries.

Stable isotope ratios of carbon ( $\delta^{13}\text{C}$ ) and nitrogen ( $\delta^{15}\text{N}$ ) have been widely used to examine the trophic ecology and migrations of marine organisms (Fry, 2006). In particular,  $\delta^{15}\text{N}$  values are used to estimate the trophic position (TP) of consumers, and food chain length when communities are assessed (Hunt et al., 2015). To calculate a TP, the consumer  $\delta^{15}\text{N}$  values must be corrected for the  $\delta^{15}\text{N}$  value at the base of marine food webs (i.e., the isotopic baseline, Graham et al., 2010) and by an averaged trophic enrichment factor (TEF) between the consumer and its prey (Minagawa and Wada, 1984; Post, 2002). This nitrogen (N) isotopic baseline can show large spatial and temporal variations due to variability in the dominant dissolved N species present, demand for the nitrogenous nutrients by primary producers, and N biogeochemical cycling (Lorrain et al., 2015). For example, water column denitrification has a large isotope effect of 25–30‰, which increases the  $\delta^{15}\text{N}$  value of all organisms in areas where this process is important (Sigman et al., 2009). By contrast, dinitrogen ( $\text{N}_2$ ) fixation has a small isotope effect and produces sea surface particulate organic matter (POM)  $\delta^{15}\text{N}$  values close to 0‰ (Sigman et al., 2009).

To determine the TP of top predators over a broad spatial scale, it is necessary to know the spatial variability of the  $\delta^{15}\text{N}$  values of the ecosystem baseline. Few detailed maps of measured  $\delta^{15}\text{N}$  baseline values, or isoscapes, are available in oceanic waters (e.g., Olson

et al., 2010), with the most comprehensive provided by McMahon et al. (2013) on zooplankton but with no data for the Western and Central Pacific Ocean. The isotopic baseline can be derived from primary producers, POM, or by primary consumers such as zooplankton or barnacles (see Lorrain et al., 2015 for a review). Biogeochemical models can also be used to provide baseline  $\delta^{15}\text{N}$  estimates (Somes et al., 2010; Navarro et al., 2013; Young et al., 2015). Finally, amino acid compound-specific  $\delta^{15}\text{N}$  analysis (AA-CSIA) has been used to account for baseline effects and produce measures of a consumer's TP (e.g., Choy et al., 2015). Within a consumer, the  $\delta^{15}\text{N}$  values of individual source AAs (e.g., phenylalanine and glycine) track  $\delta^{15}\text{N}$  values at the base of the food web (McClelland and Montoya, 2002; Popp et al., 2007; Hannides et al., 2009) while trophic AAs (e.g., glutamic acid, alanine) fractionate predictably with each trophic level. Subtraction of source from trophic AA values allows TP to be estimated using known enrichment factors between these AAs (Popp et al., 2007; Hannides et al., 2009; Nielsen et al., 2015).

In the Western and Central Pacific Ocean, large spatial variations in the POM  $\delta^{15}\text{N}$  values have been observed along a trans-Pacific transect from South America to Australia at 17°S (Shiozaki et al., 2014). Active  $\text{N}_2$  fixation from diazotrophs have been proposed to explain the lower report of POM  $\delta^{15}\text{N}$  values in the South-Western Pacific Ocean (~0‰) compared to the higher POM  $\delta^{15}\text{N}$  values in the Eastern Pacific Ocean (Shiozaki et al., 2014). By combining two stable isotope techniques (bulk  $\delta^{15}\text{N}$  analysis and AA-CSIA), the main aim of this study was to provide tuna TP estimates accounting for isotopic baseline variability. We analyzed the  $\delta^{15}\text{N}$  values of bulk tissues and individual amino acids of two commercially important tropical tuna species: bigeye (*Thunnus obesus*) and yellowfin (*Thunnus albacares*), and compiled a large dataset for POM  $\delta^{15}\text{N}$  values within the Western and Central Pacific Ocean. The specific aims of this study were to: (i) generate fine-scale  $\delta^{15}\text{N}$  isoscapes and identify spatial patterns in POM, tuna bulk muscle  $\delta^{15}\text{N}$  values and TP estimates, (ii) provide and compare TP estimates based on bulk POM  $\delta^{15}\text{N}$  values and AA  $\delta^{15}\text{N}$  of tuna muscle, and (iii) examine the influence of environmental and biological variables on tuna TP across the Western and Central Pacific Ocean using a generalized additive model (GAM). Tagging data for bigeye were also used to validate the generated hypotheses regarding vertical and horizontal habitats.

## 2. Methods

### 2.1. Sample collection

White muscle tissue samples (n = 1039) were collected from 416 bigeye and 623 yellowfin tuna within the Western and Central Pacific Ocean between 2001 and 2015. Sample collection was performed onboard commercial fishing boats (purse seine and long-line) by scientific observers. Tuna were captured from 138°E to 140°W and from 10°N to 26°S covering the different biogeographical provinces defined by Longhurst, 2007 (Fig. 1). Fork length (FL) was measured to the nearest cm for each tuna, and white muscle samples were extracted from the anal fin region. Tuna FL range was 19–175 cm (84 ± 33 cm; mean ± SD) and 27–160 cm (101 ± 33 cm) for bigeye and yellowfin tuna, respectively. Samples were then kept frozen at –20°C and freeze-dried before analyses. Bulk  $\delta^{15}\text{N}$  analysis was performed on all samples and a subset of 16 individuals (10 bigeye from 2012 to 2013 and 6 yellowfin from 2003, 2010 and 2013) were analyzed for AA-CSIA (Fig. 1). This subset of 16 individuals was composed of tuna of similar sizes (110 ± 11 cm and 109 ± 23 cm for bigeye and yellowfin tuna, respectively). Their  $\delta^{15}\text{N}$  values were representative of the mean value of other tuna in the same region (Tables S1 and S2). Five

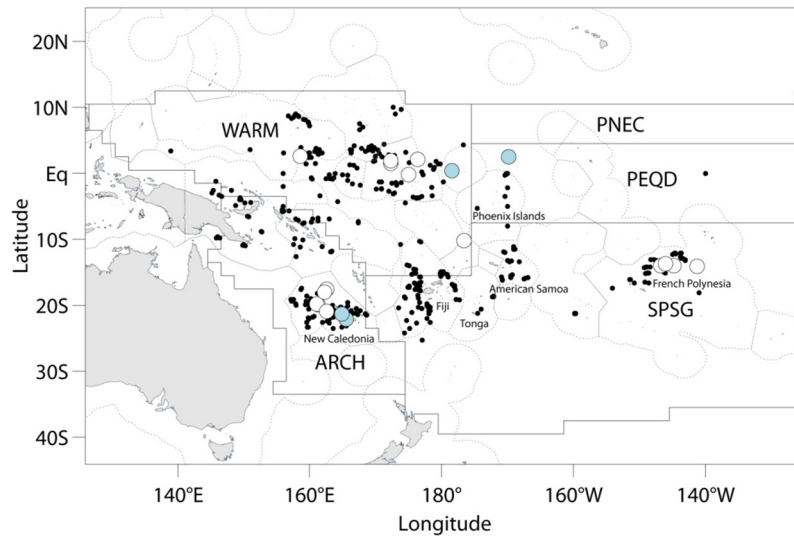


**Fig. 1.** Tuna sampling locations for bulk  $\delta^{15}\text{N}$  analyses (black dots), amino acid compound-specific  $\delta^{15}\text{N}$  analysis (white dots) and archival tags (blue dots). Black lines delineate Longhurst biogeographical provinces: Warm Pool (WARM), Pacific Equatorial Divergence (PEQD), Archipelagic Deep Basins (ARCH), North Pacific Equatorial Counter Current (PNEC), South Pacific Subtropical Gyre (SPSG) (Longhurst, 2007). Grey lines represent the exclusive economic zones. (For interpretation of the references to color in this figure legend, the reader is referred to the web version of this article.)

supplementary yellowfin AA  $\delta^{15}\text{N}$  values (from 2002 to 2003) from Lorrain et al. (2015) were added to the dataset (Fig. 1).

Samples of POM were collected from different oceanic research cruises in the Western and Central Pacific Ocean (Table 1). Surface seawater (4–10 L) was filtered through pre-combusted GF/F filters (porosity 0.7  $\mu\text{m}$ ). Samples were stored frozen at  $-20^\circ\text{C}$  prior to bulk  $\delta^{15}\text{N}$  analysis. POM  $\delta^{15}\text{N}$  data from published literature were added to our dataset to improve the spatial coverage of the POM  $\delta^{15}\text{N}$  isoscape (Altabet, 2001; Gaston and Suthers, 2004; Baird

et al., 2008; Raimbault et al., 2008; Shiozaki et al., 2014; Lorrain et al., 2015).

## 2.2. Bulk and compound-specific stable isotope analysis

Each freeze-dried tuna muscle sample was ground to powder, homogenized and analyzed for  $\delta^{15}\text{N}$  and % N. The bulk  $\delta^{15}\text{N}$  values were determined using an elemental analyzer (Flash 2000, Thermo Scientific, Milan, Italy) coupled to an isotope ratio mass

**Table 1**

Particulate organic matter  $\delta^{15}\text{N}$  values by biochemical region delineated in this study and by cruise date (mean  $\pm$  SD). The mean values for each biochemical region are in bold characters.

Biochemical regions	$\delta^{15}\text{N}$ (mean $\pm$ SD)	n	Date	References
WARMm	$6.2 \pm 1.6\text{‰}$	10	Jul-12	This study
	$5.8 \pm 1.7\text{‰}$	5	Feb-13	This study
	$6.7 \pm 4.8\text{‰}$	7	Mar-14	This study
	$8.9 \pm 1.7\text{‰}$	18	Jul–Aug 15	This study
	<b><math>7.5 \pm 2.7\text{‰}</math></b>	<b>40</b>		
PEQD	$1.7 \pm 0.5\text{‰}$	4	Aug-92	Altabet, 2001
	$5.5 \pm 0.7\text{‰}$	2	Nov-04	Raimbault et al. (2008)
	$0.8 \pm 2.1\text{‰}$	8	Mar-05	Lorrain et al. (2015)
	<b><math>1.7 \pm 2.3\text{‰}</math></b>	<b>14</b>		
ARCHm	$0.0 \pm 2.0\text{‰}$	30	Apr–Jul 09	Shiozaki et al. (2014)
	$6.5 \pm 0.3\text{‰}$	2	Jul-12	This study
	$3.5 \pm 2.1\text{‰}$	11	Feb-13	This study
	$2.7 \pm 3.0\text{‰}$	13	Feb–Apr 15	This study
	$3.2 \pm 1.3\text{‰}$	4	Oct-15	This study
	$4.6 \pm 1.4\text{‰}$	4	Dec-15	This study
	<b><math>1.9 \pm 3.0\text{‰}</math></b>	<b>64</b>		
SPSGm	$14.0\text{‰}$	1	Aug-92	Altabet (2001)
	$11.0 \pm 2.9\text{‰}$	39	Apr–Jul 09	Shiozaki et al. (2014)
	<b><math>11.1 \pm 2.9\text{‰}</math></b>	<b>40</b>		
PNEC	$7.5 \pm 0.6\text{‰}$	2	Aug-92	Altabet (2001)
	$7.8 \pm 2.0\text{‰}$	5	Mar-05	Lorrain et al. (2015)
	<b><math>7.7 \pm 1.6\text{‰}</math></b>	<b>7</b>		

WARMm = Warm Pool modified; PEQD = Pacific Equatorial Divergence; ARCHm = Archipelagic Deep Basins modified; SPSGm = South Pacific Subtropical Gyre modified; PNEC = North Pacific Equatorial Counter Current.

spectrometer (Delta V Plus with a ConFlo IV interface, Thermo Scientific, Bremen, Germany). Stable isotope values are reported in standard  $\delta$ -notation relative to atmospheric  $N_2$ . Repeated analyses of laboratory reference materials with C/N values similar to tuna muscle tissue indicated that the precision and accuracy of the bulk isotopic measurements was  $<0.2\%$ . In addition, the precision in the  $\delta^{15}N$  values of several sample tissues measured in triplicate was  $<0.2\%$ . Values are reported as means  $\pm$  SD. For AA-CSIA, freeze-dried tuna samples were prepared by acid hydrolysis followed by derivatization to produce trifluoroacetic amino acid esters using standard methods (Popp et al., 2007). The nitrogen isotopic compositions of the trifluoroacetic amino acid esters derivatives of amino acids (glycine, phenylalanine, alanine, glutamic acid, leucine and proline) were analyzed using a Delta V Plus mass spectrometer interfaced with an Ultra Trace GC gas chromatograph through a GC IsoLink combustion furnace, and liquid nitrogen cold trap (Thermo Fisher Scientific, Germany) at the National Institute of Water and Atmospheric (NIWA, New Zealand) research institute's stable isotope ecological laboratory. Measured isotopic compositions were corrected relative to known  $\delta^{15}N$  values for internal reference material (i.e., caffeine and leucine). All samples were analyzed at least in triplicate. The average standard deviation of the multiple analyses per amino acid was  $0.9\%$ , ranging from  $0.01\%$  to  $3.3\%$ .

### 2.3. Contour maps

A generalized additive model (GAM) was used to generate smoothed spatial contour maps of observed POM  $\delta^{15}N$  values, tuna  $\delta^{15}N$  values and tuna TP estimates. A GAM is a semi-parametric approach that is able to extract flexible non-linear features in the data through a function of non-parametric smooth functions (Hastie and Tibshirani, 1990):

$$E(Y) = \beta_0 + \beta_1(x_1) + f_2(x_2) + f_3(x_3) + \dots$$

where  $Y$  is a response variable that belongs to an exponential family distribution,  $\beta_0$  is the intercept,  $\beta_1$  is an (optional) parametric regression coefficient and  $f_k(x_k)$  is a smooth function of the covariate  $x_k$ . The GAM was fitted here with the `gam()` function using the “mgcv” package (Wood, 2006) in R (R Core Team, 2016) and assuming a normal error distribution.

To produce a spatially interpolated contour map of POM  $\delta^{15}N$  values, two dimensional thin plate regression splines were fitted to the samples by location using the structure  $s(\text{longitude}, \text{latitude})$ . The resulting POM  $\delta^{15}N$  contour map (i.e., isoscape) was then examined to identify different biochemical regions within the Western and Central Pacific Ocean, as characterized by distinct  $\delta^{15}N$  values. A coarser spatial interpolation at the  $7.5^\circ$  resolution was also applied, with the grid centered on the equator. The predicted values from this interpolation were used as the isotopic baseline in the subsequent analyses of tuna TP estimates (detailed below). We applied the coarser resolution here because using a POM value from a single location would unlikely be representative of that incorporated into the prey of highly-mobile top predators. The  $7.5^\circ$  value was arbitrarily chosen as a compromise between a  $5^\circ$  and  $10^\circ$  resolution. The width of a  $7.5^\circ$  grid cell at  $15^\circ S$  also approximately matches the model-estimated median lifetime displacement for yellowfin tuna, i.e., 805 km (Sibert and Hampton, 2003).

### 2.4. Trophic position estimates of tuna

The TP was first estimated from bulk tuna muscle  $\delta^{15}N$  and POM  $\delta^{15}N$  values. For each tuna species, the POM  $\delta^{15}N$  spatial interpolation at the  $7.5^\circ$  resolution was used to predict POM  $\delta^{15}N$  values at every tuna sampling location. The TP for each tuna species and each sampling location was calculated as follows:

$$TP_x = \frac{\delta^{15}N_x - \delta^{15}N_{POM}}{TEF} + TP_{baseline}$$

where  $x$  is the studied species and TEF is the trophic enrichment factor between trophic levels, set at 2.4 following Olson et al. (2010) and Lorrain et al. (2015), and derived from Vanderklift and Ponsard (2003). A  $TP_{baseline}$  of 1 was used for surface POM. Contour maps of the resulting tuna TP estimates were generated using a two-dimensional GAM as outlined above. To compare TP estimates among biochemical regions, non-parametric Kruskal-Wallis tests were used with Mann-Whitney *post hoc* test in R (significant level set to 0.01).

The TP of tuna was also estimated using the difference in tuna  $\delta^{15}N$  values of source (Sr-AA) and trophic (Tr-AA) amino acids. Those values were calculated using the weighted mean of specific suites of AAs that were present in all samples analyzed using the following equation:

$$TP_{Tr-Sr} = \frac{\delta^{15}N_{Tr-AA} - \delta^{15}N_{Sr-AA} - \beta_{Tr-Sr}}{TEF_{Tr-Sr}} + 1$$

where  $\delta^{15}N_{Sr-AA}$  is the weighted average of glycine, and phenylalanine  $\delta^{15}N_{AA}$  values, and  $\delta^{15}N_{Tr-AA}$  is the weighted average of alanine, glutamic acid, leucine, and proline  $\delta^{15}N_{AA}$  values.  $\beta_{Tr-Sr}$  is the difference between trophic and source AAs in primary producers and  $TEF_{Tr-Sr}$ , the  $^{15}N$  enrichment between Tr-AA and Sr-AA per TP. A  $\beta_{Tr-Sr}$  of 3.6 and a  $TEF_{Tr-Sr}$  of 5.7 were used (Bradley et al., 2014; Choy et al., 2015). Using the weighted mean of Sr-AA and Tr-AA reduces uncertainty due to the possible large variation of  $\delta^{15}N_{AA}$  values (Hayes et al., 1990).

To compare TP estimates from bulk and AA  $\delta^{15}N$  values, we averaged TP estimates from bulk tissue  $\delta^{15}N$  values in a square of  $7.5^\circ$  centered on each AA sample location. All values are expressed as means  $\pm$  SD.

### 2.5. Biological and oceanographic drivers of tuna TP estimates

A GAM was applied to examine the relationships among tuna TP estimates and explanatory variables including both biological (FL) and environmental parameters known to impact tuna habitat (e.g., Brill, 1994; Evans et al., 2008). The environmental parameters selected were from the following datasets: (1) observed monthly mean sea surface temperature (SST in  $^\circ C$ ) from the National Oceanic and Atmospheric Administration (NOAA, <https://www.ncdc.noaa.gov/oisst>; Reynolds et al., 2002) on a  $1^\circ \times 1^\circ$  grid, (2) monthly means of net primary production (NPP in  $mg\ C\ m^{-2}\ d^{-1}$ ) from a vertically generalized production model (VGPM, <http://www.science.oregonstate.edu/ocean.productivity>; Behrenfeld and Falkowski, 1997) available at a 9 km resolution which we interpolated onto a  $1^\circ \times 1^\circ$  grid for coherency with SST, (3) the depth of the  $20^\circ C$  isotherm (used a thermocline proxy, referred to as d20 in m) and the depth of the  $12^\circ C$  isotherm (d12) calculated from  $1^\circ \times 1^\circ$  monthly ARGO data ([http://www.argo.ucsd.edu/Gridded\\_fields.html](http://www.argo.ucsd.edu/Gridded_fields.html)), and (4) the depth of the  $160\ \mu M$  (i.e.,  $3.5\ ml\ l^{-1}$ )  $O_2$  isopleth (referred to as d160 in m), calculated from  $1^\circ \times 1^\circ$  monthly climatology from World Ocean Atlas data (<https://www.nodc.noaa.gov/OC5/woa13>; Garcia et al., 2013). Because the tuna data analyzed cover the 2001–2015 time period with an important number of observations before 2004, we computed the monthly climatology from the inter-annual d20 and d12. For each tuna sample location, these oceanographic variables were then averaged over a six month period preceding the capture date to take into account the tuna muscle  $^{15}N$  turnover rate (half life = 167 days; Madigan et al., 2012).

Explanatory variables that were shown to make a significant contribution to the model were fitted with thin-plate regression splines and a low spline complexity (knot = 3) to reduce

over-fitting. A backward model selection approach was used. We did not account for temporal effects as the sampling was uneven across time. We evaluated model assumptions by checking the normality of model residuals as well as selecting for smaller generalized cross-validation values (GCV; Wood, 2006). The contribution of each variable to the final model was tested by evaluating the drop in deviance explained (drop-contribution) by the model when the variable was removed, with variables showing a high drop-contribution assigned a greater explanatory rank (Castella et al., 2001; Gallardo et al., 2009) (see also Table S3 for the deviance explained when the variables are used as the sole explanatory variable in the model).

### 2.6. Tagging data for bigeye tuna

Tracking data from both archival tags and pop-up satellite tags were extracted from the large scale Pacific Tuna Tagging Programme (see Leroy et al., 2013). We specifically selected 4 large adult bigeye tuna (~100 cm) with enough days at liberty (>2 months) and with sizes and movements that fell within the bounds of our tuna sample coverage, targeting fish from the PEQD, WARM, and ARCH biogeographical provinces. The bigeye tuna were tagged at 2 different locations (Fig. 1): two at the equator (Phoenix Islands, in the PEQD and WARM Longhurst biogeographical provinces, archival tags Mk9, manufactured by Wildlife Computers, Redmond, WA, USA) and two off New Caledonia (in the ARCH Longhurst biogeographical province, pop-up satellite archival tags PAT-4, Wildlife Computers, Redmond, USA). The depth (pressure), ambient temperatures, and light-level data were recorded at frequencies of either 30 or 60 s. The materials and methods used for tagging and releasing bigeye tuna with archival tags are described by Schaefer and Fuller (2002). Estimated daily positions for each tag were derived from the UKFsst model (Nielsen et al., 2006) or from the state-space model described in Nielsen and Sibert (2007) implemented in the R software package “trackit” ([www.soest.hawaii.edu/tag-data/trackit](http://www.soest.hawaii.edu/tag-data/trackit)). Recorded temperature and depth time series data were used to examine the vertical movement behavior of each fish. Mean day and night depths show where fish species spend most of their time on average during daylight and night hours, excluding dawn and dusk, with 7:00–17:00 for daylight hours and 19:00–5:00 (UTC + 11:00) for night hours.

## 3. Results

### 3.1. POM $\delta^{15}\text{N}$ spatial variability

The spatial GAM used to generate the POM  $\delta^{15}\text{N}$  isoscape demonstrated strong spatial trends in the distribution of POM  $\delta^{15}\text{N}$  values (with 74.4% of variance explained). According to these observed  $\delta^{15}\text{N}$  spatial patterns and considering the strong similarity with the biogeographical provinces defined by Longhurst (2007) (Fig. 1), we delimited 5 biochemical regions named after Longhurst’s nomenclature: “Warm Pool modified” (WARMm), “Pacific Equatorial Divergence” (PEQD), “South Pacific Subtropical Gyre modified” (SPSGm), “North Pacific Equatorial Counter Current” (PNEC), and “Archipelagic Deep Basins modified” (ARCHm) (Fig. 2). The longitudinal delimitation of WARMm, SPSGm and ARCHm biochemical regions being slightly different from Longhurst (2007), they were denoted “modified”. The ARCHm biochemical region from 10°S to 25°S was characterized by low POM  $\delta^{15}\text{N}$  values ( $1.9 \pm 3.0\text{‰}$ , Fig. 2, Table 1). Along the 20°S transect, POM  $\delta^{15}\text{N}$  values then increased eastward from ARCHm to reach a maximum in SPSGm ( $11.1 \pm 2.9\text{‰}$ ). In the eastern part of our study area, POM  $\delta^{15}\text{N}$  showed a clear latitudinal gradient with val-

ues lowest at the equator in the PEQD ( $1.7 \pm 2.3\text{‰}$ ) and increasing poleward to SPSGm ( $11.1 \pm 2.9\text{‰}$ ) and PNEC ( $7.7 \pm 1.6\text{‰}$ ). Finally, the north-western part of the studied area from 10°S to 7°N showed intermediate  $\delta^{15}\text{N}$  values ( $7.5 \pm 2.7\text{‰}$ ).

### 3.2. Tuna $\delta^{15}\text{N}$ values

Observed averaged tuna  $\delta^{15}\text{N}$  values over the entire study area were  $14.7 \pm 3.0\text{‰}$  and  $12.6 \pm 3.0\text{‰}$  for bigeye and yellowfin tuna, respectively (range 8.4–23.1‰ for bigeye and 7.9–21.5‰ for yellowfin). The spatial GAM, including latitude and longitude, explained 73.6% and 63.0% of variability in  $\delta^{15}\text{N}$  values of bigeye and yellowfin tuna, respectively (Fig. 3). All tuna species exhibited strong spatial gradients in  $\delta^{15}\text{N}$  values with similar patterns displayed among the 2 species (fitted maps; Fig. 3). Maximum  $\delta^{15}\text{N}$  values were found in the south-east in SPSGm ( $19.4 \pm 2.5\text{‰}$  and  $17.2 \pm 2.6\text{‰}$  for bigeye and yellowfin tuna, respectively), while minimum values were recorded in the south-west off New Caledonia, Fiji and Tonga in ARCHm ( $12.5 \pm 1.8\text{‰}$  and  $10.9 \pm 2.0\text{‰}$  for bigeye and yellowfin tuna, respectively). Intermediate values were found at the equator in WARMm ( $15.5 \pm 1.7\text{‰}$  and  $14.1 \pm 2.5\text{‰}$  for bigeye and yellowfin tuna, respectively). Finally bigeye and yellowfin tuna showed low  $\delta^{15}\text{N}$  values in PEQD ( $12.1 \pm 1.6\text{‰}$  and  $13.0 \pm 2.6\text{‰}$ , respectively). No tuna were sampled in PNEC.

### 3.3. Trophic position estimates

Tuna TP estimated from POM  $\delta^{15}\text{N}$  values averaged  $4.6 \pm 1.1$  (range 1.9–8.1) and  $4.3 \pm 1.1$  (range 1.5–8.2) over the entire study area for bigeye and yellowfin tuna, respectively. The spatial GAM, including latitude and longitude, explained 64.8% and 51.4% of bigeye and yellowfin tuna  $\delta^{15}\text{N}$  variability, respectively (Fig. 4). Contour maps of TP estimates showed a consistent latitudinal trend for bigeye and to a lesser extent yellowfin, with lower TP estimates (by ~1) above ~5°S–10°S compared to southern latitudes from 10 to 25°S. The highest TP estimates for the 2 tuna species were observed in ARCHm around Fiji at 180°W from 10°S to 25°S, and at 150°W–10°S in the western part of French Polynesia (SPSGm). According to biochemical regions, mean TP estimates for bigeye were  $5.6 \pm 0.8$ ,  $5.4 \pm 1.1$ ,  $4.1 \pm 0.8$  and  $3.7 \pm 0.8$  in ARCHm, SPSGm, WARMm and PEQD, respectively (Table 2; Fig. S1). Mean TP estimates for yellowfin were  $4.8 \pm 0.9$ ,  $4.6 \pm 1.1$ ,  $3.6 \pm 1.1$  and  $3.7 \pm 0.9$  in ARCHm, SPSGm, WARMm and PEQD, respectively. Bigeye and yellowfin tuna had significantly lower TP values in biochemical regions above ~10°S (i.e., WARMm and PEQD) compared to those at higher southern latitudes (i.e., ARCHm and SPSGm; Fig. S1).

Based on AA-CSIA, bigeye TP estimates varied considerably over the study area with mean values of  $5.0 \pm 0.8$  and  $4.8 \pm 1.0$  in ARCHm and SPSGm, respectively and lower TP estimates of  $4.0 \pm 1.1$  in WARMm (Fig. 5B, Table S1). Over the same biochemical regions, there was a small spatial difference for yellowfin TP only between ARCHm and other regions with mean estimates of  $4.3 \pm 0.7$  in ARCHm vs.  $3.9 \pm 0.6$  and  $4.1 \pm 0.9$  in SPSGm and WARMm, respectively.

The comparison of the spatial trends of tuna TP estimated from both methods (AA-CSIA vs. bulk  $\delta^{15}\text{N}$  analysis, Fig. 5) showed similar results for bigeye but slightly different for yellowfin tuna, with AA-CSIA showing slightly higher TP estimates in ARCHm (but not in SPSGm) compared to WARMm.

### 3.4. Drivers of tuna TP estimates

The GAM that produced the highest variance explained included the depth of the 20°C isotherm (d20), fork length (FL), SST and the depth of the 160  $\mu\text{M}$   $\text{O}_2$  isopleth (d160) for bigeye

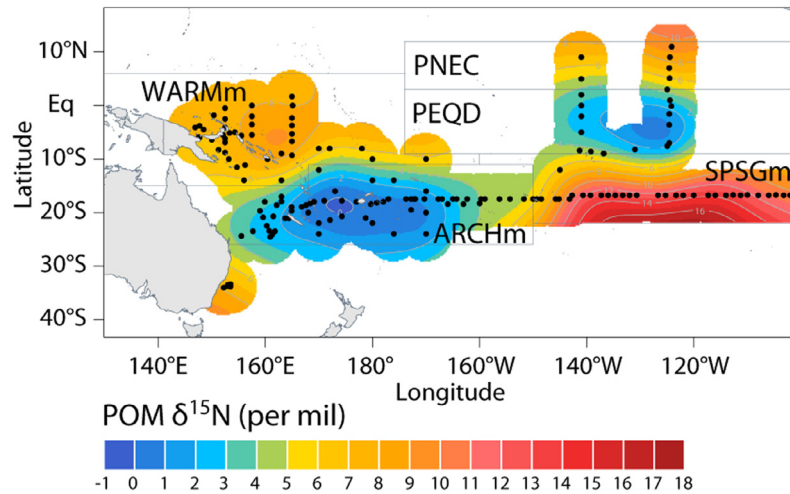


**Fig. 2.** Central and Western Pacific particulate organic matter (POM)  $\delta^{15}\text{N}$  isoscape from a spatially derived generalized additive model. The black dots represent POM sample locations and the grey lines delineate the 5 biochemical regions based on distinct POM  $\delta^{15}\text{N}$  values: WARMm (Warm Pool modified), PEQD (Pacific Equatorial Divergence), SPSGm (South Pacific Subtropical Gyre modified), PNEC (North Pacific Equatorial Counter Current) and ARCHm (Archipelagic deep basins modified). (For interpretation of the references to color in this figure legend, the reader is referred to the web version of this article.)

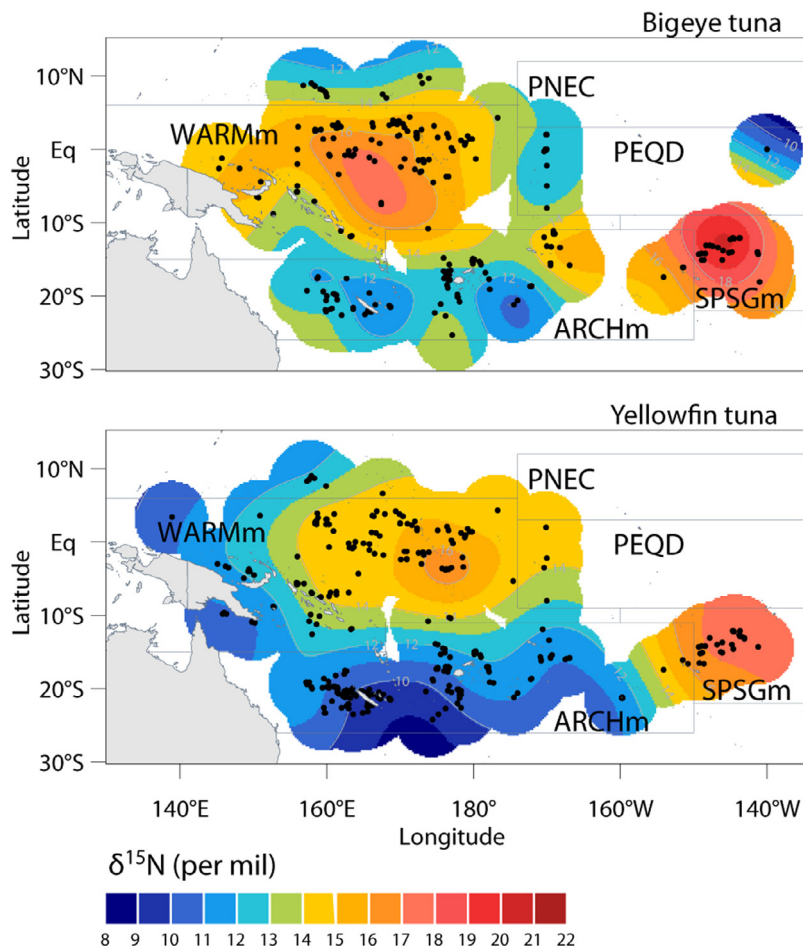


**Fig. 3.** Bulk  $\delta^{15}\text{N}$  isoscapes for bigeye and yellowfin tuna in the Western and Central Pacific Ocean from a spatially derived generalized additive model. The black dots represent tuna sample locations and the grey lines delineate the biochemical regions based on distinct particulate organic matter  $\delta^{15}\text{N}$  values: WARMm (Warm Pool modified), PEQD (Pacific Equatorial Divergence), SPSGm (South Pacific Subtropical Gyre modified), PNEC (North Pacific Equatorial Counter Current) and ARCHm (Archipelagic deep basins modified). (For interpretation of the references to color in this figure legend, the reader is referred to the web version of this article.)

and yellowfin tuna (Table 3). The depth of the 12°C and 20°C isotherms had similar explanatory power for both species but the per-

formance of the 12°C was poorer for yellowfin (Table S3). Given that those two variables are collinear over much of our study area,

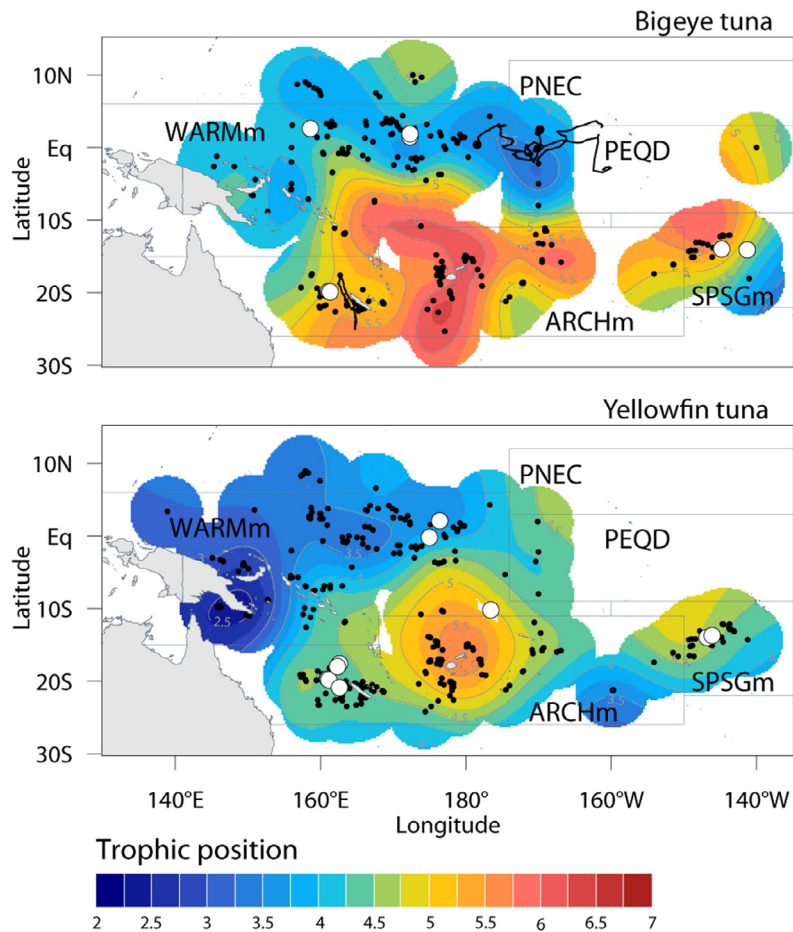


**Fig. 4.** Contour map of trophic positions estimated from bulk  $\delta^{15}\text{N}$  values for bigeye and yellowfin tuna within the Western and Central Pacific Ocean. Tuna sampling locations for bulk  $\delta^{15}\text{N}$  analysis (black dots) and for amino acid compound-specific isotope  $\delta^{15}\text{N}$  analysis (white dots) are indicated. Most probable tracks for the four tagged bigeye tuna are represented by black lines. Grey lines delineate the 5 biochemical regions: WARMm (Warm Pool modified), PEQD (Pacific Equatorial Divergence), SPSGm (South Pacific Subtropical Gyre modified), PNEC (North Pacific Equatorial Counter Current) and ARCHm (Archipelagic Deep Basins modified). (For interpretation of the references to color in this figure legend, the reader is referred to the web version of this article.)

**Table 2**

Trophic position (TP) estimates for bigeye and yellowfin tuna from bulk  $\delta^{15}\text{N}$  analysis within biochemical regions delineated in this study for the Western and Central Pacific Ocean. Kruskal-Wallis test with Mann-Whitney *post hoc* tests were used to assess difference in TP estimates between biochemical regions. Regions sharing the same letter are not statistically different.

Species	Biochemical regions	Bulk $\delta^{15}\text{N}$ values		
		n	TP (mean $\pm$ SD)	Post-hoc test
Bigeye tuna	ARCHm	111	5.6 $\pm$ 0.8	a
	SPSGm	57	5.4 $\pm$ 1.1	a
	WARMm	178	4.1 $\pm$ 0.8	b
	PEQD	51	3.7 $\pm$ 0.8	c
Yellowfin tuna	ARCHm	327	4.8 $\pm$ 0.9	a
	SPSGm	45	4.6 $\pm$ 1.1	a
	WARMm	237	3.6 $\pm$ 1.1	b
	PEQD	5	3.7 $\pm$ 0.9	ab

WARMm = Warm Pool modified; PEQD = Pacific Equatorial Divergence; ARCHm = Archipelagic Deep Basins modified; SPSGm = South Pacific Subtropical Gyre modified; PNEC = North Pacific Equatorial Counter Current.

we elected to retain the d20 as the explanatory variable standing for thermocline depth. Net primary production was tested but was not retained in the final model selection as it explained less than 1% of TP estimates and showed limited spatial variation within most of the study region. The best GAM explained 48.6% and 33.4% of the variance for bigeye and yellowfin tuna, respectively (Table 3). Of the environmental variables, d20 was the most

effective single explanatory variable for both species explaining 16.9 and 10.3% of TP variability for bigeye and yellowfin tuna, respectively. The d20 was positively correlated with tuna TP and a rise of  $\sim 1.5$  TP and  $\sim 1$  TP, respectively, was predicted when d20 shifted from 160 m to 250 m deep (i.e., at southern latitudes; Fig. 6). The SST and FL were weaker predictors for bigeye and yellowfin, contributing an additional 4% of explained variation. The

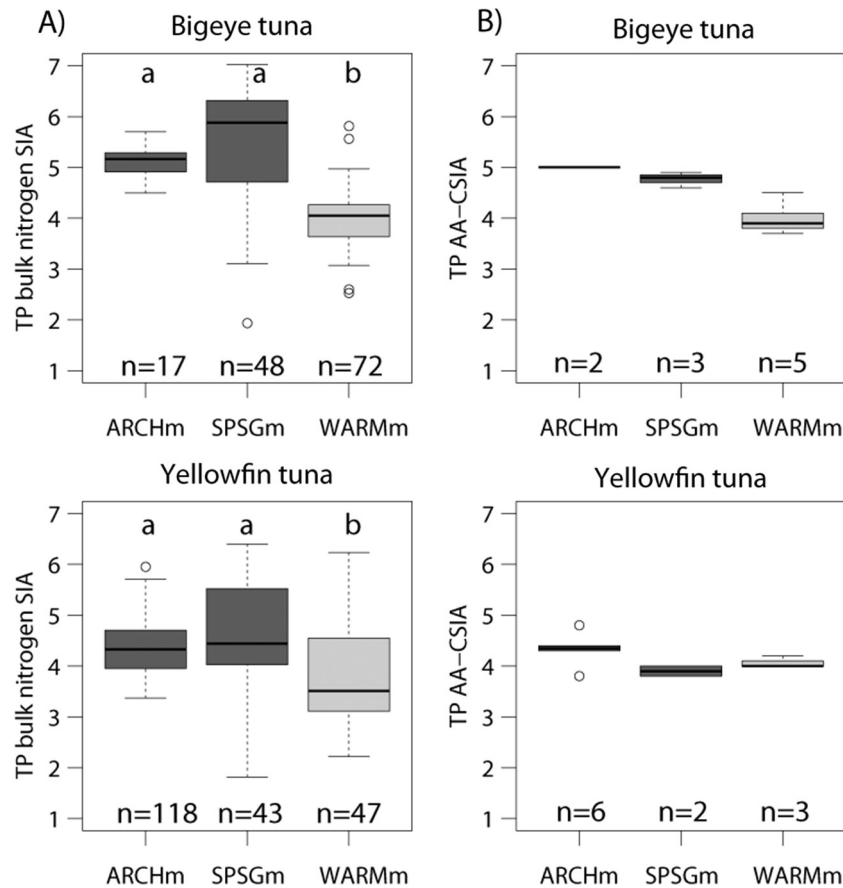


**Fig. 5.** Comparison of trophic position (TP) estimates for bigeye and yellowfin tuna from bulk  $\delta^{15}\text{N}$  analysis (A) and amino acid compound-specific  $\delta^{15}\text{N}$  analysis (AA-CSIA) (B) in the 3 biochemical regions: WARMm (Warm Pool modified), SPSGm (South Pacific Subtropical Gyre modified) and ARCHm (Archipelagic Deep Basins modified). Boxplots show the median (middle line) and the interquartile range (box). The whiskers extend to the minimum and maximum observations. Observations are shown as outlier points if they occur beyond the whiskers. Dark grey and light grey represent southern (ARCHm, SPSGm) and northern (WARMm) biochemical regions, respectively. Letters show which biochemical regions are statistically different: within the same species, regions with the same letter are not statistically different and region with different letters are statistically different.

**Table 3**

Summary of results from the best generalized additive models (GAM) applied on bigeye and yellowfin tuna trophic position estimated from bulk  $\delta^{15}\text{N}$  analysis. For each variable we included the effective degree of freedom (edf), the p-value and the deviance explained by all the predictors combined (DE).

Best GAM selected	Trophic Position		
Bigeye tuna	Intercept estimate $\pm$ SE: $4.54 \pm 0.04$		
	edf	p-value	DE (%)
s(d20, k = 3)+	1.78	$<2e-16$	48.6
s(FL, k = 3)+	1.92	$5.88e-07$	
s(SST, k = 3)+	2.00	$7.24e-07$	
s(d160, k = 3)	1.01	$1.52e-04$	
Yellowfin tuna	Intercept estimate $\pm$ SE: $4.31 \pm 0.04$		
	edf	p-value	DE (%)
s(d20, k = 3)+	1.83	$<2e-16$	33.4
s(FL, k = 3)+	1.89	$9.20e-08$	
s(SST, k = 3)+	1.97	$5.66e-08$	
s(d160, k = 3)	1.00	$3.64e-08$	

d160 was the lowest ranked environmental variable for bigeye and yellowfin tuna explaining 2.1 and 3.9% of TP estimates, respectively.

### 3.5. Bigeye tuna tagging data

The four tagged bigeye tuna displayed distinct diel pattern in depth preferences (Fig. 7). Bigeye tuna tagged in ARCHm (New

Caledonia) mostly spent daytime hours between 300 and 450 m deep, while fish tagged at WARMm and PEQD (at the equator) spent daytime hours at shallower depths, between 250 and 350 m deep. Average day time depth for tagged bigeye were 343 and 323 m at the equator and 391 and 409 m in New Caledonia (Table 4). The opposite pattern occurred at nighttime, with bigeye from WARMm and PEQD occupying deeper depths than bigeye from WARMm. Bigeye tuna experienced a wider temperature range in WARMm and PEQD ( $10\text{--}25^\circ\text{C}$ ) than those in ARCHm ( $15\text{--}25^\circ\text{C}$ ) (Table 4). However, as bigeye from the equator occupied deeper habitats during the night and shallower habitats during the day, over a 24 h cycle, all individuals experienced mean temperature close to  $19\text{--}20^\circ\text{C}$  (Table 4). Both bigeye from ARCHm remained within the New Caledonia exclusive economic zone with maximum horizontal movements of about 460 km from their release position over 60 days (Fig. 4). At the equator, both bigeye displayed eastward movements with the greatest eastward movement being  $\sim 1900$  km from their release position after 90 days (Fig. 4). Latitudinal movements were restricted with a maximum latitudinal movement of  $\sim 370$  km for all studied bigeye.

## 4. Discussion

Our study established the first data-driven baseline  $\delta^{15}\text{N}$  isoscape for the Western and Central Pacific Ocean. We proposed a delimitation of biochemical regions based on the spatial

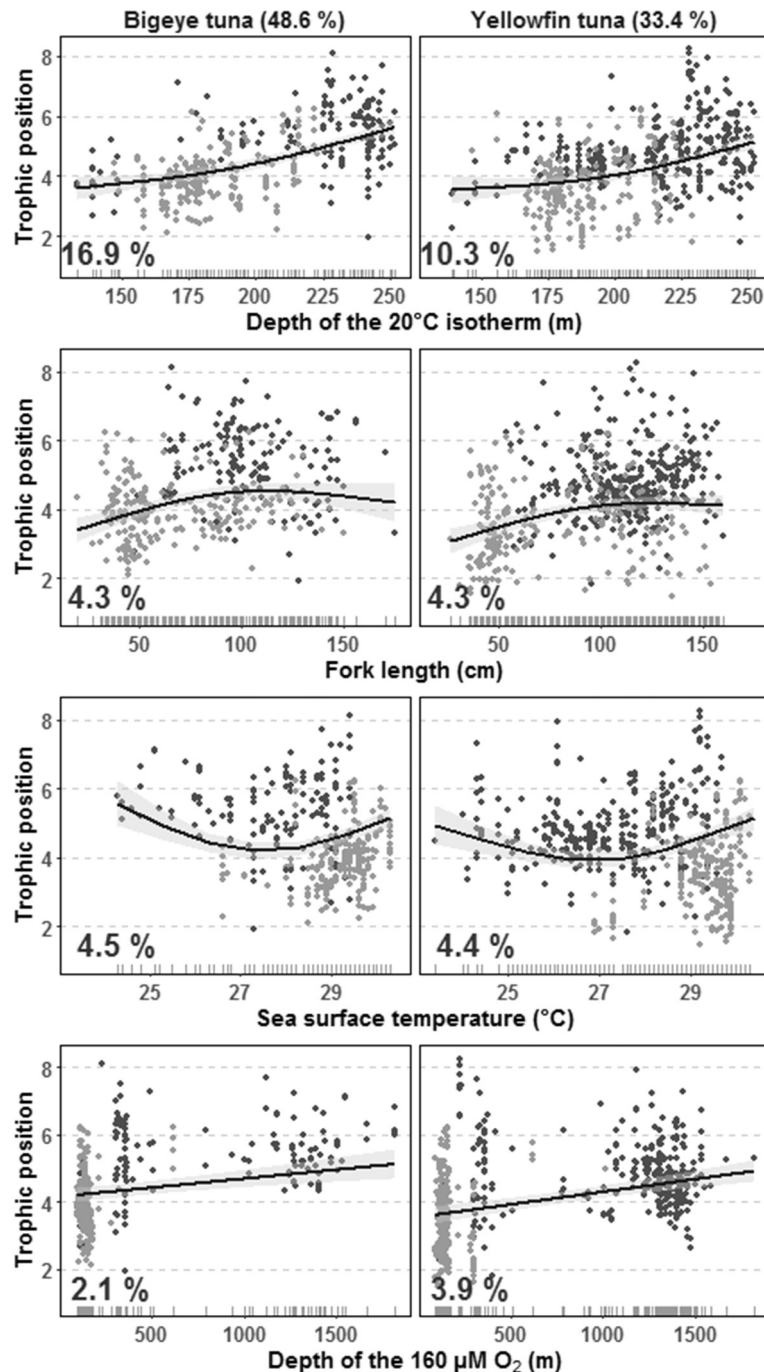


**Fig. 6.** Relationships between trophic position estimates and environmental explanatory variables for bigeye and yellowfin tuna from generalized additive models. Dark grey and light grey dots represent southern (Archipelagic Deep Basins modified, South Pacific Subtropical Gyre modified) and northern (Warm Pool modified, Pacific Equatorial Divergence) biochemical regions, respectively. The solid grey area bracketing the response curves shows the 95% confidence limits for each smoothed spline. The total % of explained deviance for the combined model for each species is indicated above, while the partial % explained deviance for each variable is indicated within their respective panel.

distribution of these POM  $\delta^{15}\text{N}$  values that reflected the previously defined Longhurst biogeographical provinces. We showed that tropical tuna  $\delta^{15}\text{N}$  values vary spatially, which, given the rate of  $^{15}\text{N}$  isotope turnover in muscle (half life = 167 days; Madigan et al., 2012), reflects some degree of regional residency, as already reported elsewhere for tropical tuna (Popp et al., 2007; Graham et al., 2010). Correcting for the baseline influence on tuna  $\delta^{15}\text{N}$  values through two separate methods (using POM and tuna bulk  $\delta^{15}\text{N}$  values, and AA-CSIA), we produced maps of tuna trophic position estimates across the Western and Central Pacific Ocean. Finally,

using a compilation of biological and environmental data, we found that the depth of the 20°C isotherm was the most important factor influencing the spatial distribution of bigeye and yellowfin trophic positions (TP) within the Western and Central Pacific Ocean, although the effect was less strong for yellowfin tuna.

#### 4.1. POM $\delta^{15}\text{N}$ spatial patterns and utilization to estimate tuna TP

Combining data from this study and previously published POM  $\delta^{15}\text{N}$  values, we generated a fine-scaled baseline  $\delta^{15}\text{N}$  isoscape

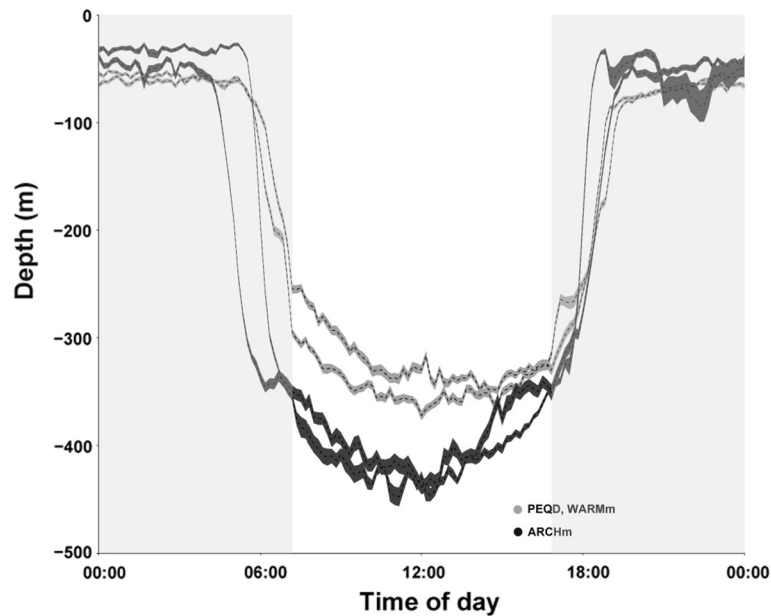


**Fig. 7.** Mean depth data with the 95% confidence interval derived from 4 bigeye tuna with archival tags by local time of day. Dark grey and light grey represent southern (Archipelagic Deep Basins modified, ARCHm) and northern (Warm Pool modified, WARMm and Pacific Equatorial Divergence, PEQD) biochemical regions. Night periods are indicated by dark grey shading.

**Table 4**

Characteristics and summary statistics of tagging data from 4 tracked bigeye tuna.

Sample ID	Biochemical region	Time period		Temperature (°C)						Depth (m)					
				Day		Night		24 h		Day		Night		24 h	
				Start	End	Mean	SD	Mean	SD	Mean	SD	Mean	SD	Mean	SD
109198	PEQD	01/12/2010	05/02/2011	11	2	24	5	19	7	-343	62	-66	37	-181	139
109337	WARMm	03/02/2011	02/05/2011	11	4	24	6	19	8	-323	82	-63	36	-181	138
40201	ARCHm	07/09/2007	15/12/2007	15	4	22	3	19	5	-391	117	-55	58	-230	181
40204	ARCHm	24/03/2005	08/05/2005	14	2	24	4	20	6	-409	88	-45	114	-215	199

WARMm = Warm Pool modified; PEQD = Pacific Equatorial Divergence; ARCHm = Archipelagic Deep Basins modified; SPStGm = South Pacific Subtropical Gyre modified; PNEC = North Pacific Equatorial Counter Current.

based on observations for the Western and Central Pacific Ocean, a region missing from the only global isoscape available (see McMahon et al., 2013). Our study revealed strong spatial patterns in POM  $\delta^{15}\text{N}$  values ( $\sim 10\text{‰}$  range) with clear gradients detected in the Western and Central Pacific Ocean  $\delta^{15}\text{N}$  isoscapes. These regional variations provided the opportunity to define several biochemical regions that are in relative agreement with Longhurst biogeographical provinces (Longhurst, 2007). The main difference was the longitudinal separation of ARCHm and SPStGm biochemical regions, with ARCHm extending further east compared to Longhurst ARCH province ( $\sim 160^\circ\text{W}$  vs.  $170^\circ\text{E}$ , i.e., a  $30^\circ$  difference). This ARCHm biochemical region is represented in our study by low POM  $\delta^{15}\text{N}$  values ( $\sim 2\text{‰}$ ) characteristic of high  $\text{N}_2$  fixation rates (Shiozaki et al., 2014).  $\text{N}_2$  fixation results in the production of organic matter with a  $\delta^{15}\text{N}$  value of  $\sim 0\text{‰}$  as diazotrophs fix the atmospheric  $\text{N}_2$  gas ( $\delta^{15}\text{N} = 0\text{‰}$ ) dissolved in seawater, with negligible isotopic fractionation (Minagawa and Wada, 1984; Altabet, 2006).

Geochemical studies (Deutsch et al., 2001; Yoshikawa et al., 2015) and direct rates measurements (Shiozaki et al., 2014; Bonnet, personal communication) report that  $\text{N}_2$  fixation is particularly active and diazotrophs particularly abundant (Campbell et al., 2005; Moisaner et al., 2010) in ARCHm compared to other regions of the Western and Central Pacific Ocean. In those studies, the influence of  $\text{N}_2$  fixation is not only observed in New Caledonia but also in Fiji and up to  $160^\circ\text{W}$ . We are therefore confident to

extend the ARCHm frontier towards the east compared to the Longhurst ARCH biogeographical province (Longhurst, 2007).

The biochemical regions outlined in this study are in accordance with known N processes fueling primary production in the Western and Central Pacific Ocean. For example in PEQD, low POM  $\delta^{15}\text{N}$  values ( $\sim 1\text{‰}$ ) were displayed but are not due to  $\text{N}_2$  fixation (Bonnet et al., 2009). In this upwelling region, low phytoplankton  $\delta^{15}\text{N}$  values should occur due to incomplete and low levels of nutrient utilization driven by Rayleigh fractionation (Altabet, 2001; Yoshikawa et al., 2006; Graham et al., 2010). For SPStGm that exhibited the highest POM  $\delta^{15}\text{N}$  values ( $\sim 11\text{‰}$ ), the nitrate pool would be completely utilized resulting in no isotope fractionation effect (Rafter et al., 2013). Finally, WARMm exhibited intermediate  $\delta^{15}\text{N}$  values ( $\sim 7\text{‰}$ ), since new primary production is mainly fueled by nitrate (Yoshikawa et al., 2006; Rafter and Sigman, 2016).

Delimitations of biochemical regions based on  $\delta^{15}\text{N}$  POM values from this study would benefit from higher temporal resolution of POM values given the seasonal variability reported in the literature (Rolf, 2000; Dore et al., 2002). In particular, the east–west and north–south limits of these biochemical regions are temporally dynamic, and robust POM estimates require multiple sampling cruises over different seasons and years. For example, our POM isoscape in SPStGm (between  $160^\circ\text{W}$  and  $100^\circ\text{W}$ ) was based on results from only one cruise and must be interpreted with caution. Nevertheless, our results provide novel and comprehensive insights into

spatial  $\delta^{15}\text{N}$  variations at the base of the food web in the Western and Central Pacific Ocean.

#### 4.2. Tuna $\delta^{15}\text{N}$ patterns and tuna movement

Tuna bulk muscle  $\delta^{15}\text{N}$  values showed strong spatial trends in the Western and Central Pacific Ocean, varying as much as 10‰ on average in accordance with previous work across comparable geographical scales (Graham et al., 2010). A high degree of spatial similarity was observed among the two tuna species and POM  $\delta^{15}\text{N}$  values. Such trends in tuna bulk  $\delta^{15}\text{N}$  values are only possible if tuna movements are restricted at the scale of their muscle nitrogen turnover rate (i.e., half life = 167 days–5.6 months; Madigan et al., 2012). These isotope-based results are corroborated by the tuna tagging data, which showed for a three month period a maximum longitudinal bigeye movement of ~1900 km at the equator, and ~460 km for the two bigeye from ARCHm (New Caledonia). According to both tagging and isotopic data, bigeye seemed to display restricted latitudinal migration at the equator which is in accordance with Schaefer et al. (2015). Previous tuna tagging studies have demonstrated that the majority of Pacific tropical movements were restricted to ca. 1852 km radius from their release locations (Hampton and Gunn, 1998; Evans et al., 2008; Schaefer and Fuller, 2010; Schaefer et al., 2015) and showed a high rate of fidelity to their tagging areas (Fonteneau and Hallier, 2015). Specifically, 47 tagged bigeye from the equatorial region demonstrated constrained latitudinal dispersion between about 8°N and 5°S as well as some regional fidelity (Fuller et al., 2015).

#### 4.3. Spatial variations of tuna TP estimates

A consistent latitudinal gradient of TP estimates from bulk analyses was observed for bigeye and yellowfin tuna within the Western and Central Pacific Ocean, with TP estimates increasing by 1–1.5 TP from ~8°N to ~25°S. This latitudinal pattern was corroborated by the AA-CSIA for bigeye but only to a lesser extent for yellowfin tuna. Other studies using bulk  $\delta^{15}\text{N}$  analyses and AA-CSIA datasets did not show any spatial TP shift for yellowfin tuna over large regions in the Indian and Pacific Ocean (Ménard et al., 2007; Popp et al., 2007; Lorrain et al., 2015; Hetherington et al., 2016). However, Olson et al. (2010) observed a higher TP for offshore yellowfin tuna compared to inshore yellowfin tuna in the Eastern Pacific Ocean. Additional AA-CSIA on yellowfin tuna is therefore required to confirm the TP latitudinal patterns for this species, especially given the high individual variability in our data and the range of years sampled for this species.

Spatial variations in the TP of tuna, as detected in this study, could result from i) differences in the structure of the lower trophic levels of the regional food webs or ii) differences in tuna diet.

The size of primary producers fundamentally influences the length of food chains (Le Borgne et al., 2011; Hunt et al., 2015). In oligotrophic waters where  $\text{N}_2$  fixation occurs (i.e., ARCHm), the presence of picophytoplankton (such as diazotrophs) favors mesozooplankton as an extra step in the food chain (Sommer et al., 2002; Gutiérrez-Rodríguez et al., 2014). By contrast, in regions where new primary production is fueled by nitrate, large phytoplankton such as diatoms are directly grazed by macrozooplankton, leading to a “shorter” food chain (Le Borgne et al., 2011). With a similar diet, tuna would have a different TP according to the structure and function of the lower trophic levels and the length of the food chain. Changes occurring at the base of the food web should affect the TP of all the tuna species equally if they reside in the region for the same period of time. As a result, clear spatial difference in TP estimates would be expected between ARCHm (Southwest region) where high  $\text{N}_2$  fixation rates have been observed compared to the other biochemical regions where  $\text{N}_2$  fix-

ation is low (e.g., SPSGm; Deutsch et al., 2001; Shiozaki et al., 2014). As the bulk  $\delta^{15}\text{N}$  analyses and AA-CSIA data showed no clear difference in tuna TP estimates between ARCHm and SPSGm, we conclude that differences in the structure and complexity of the base of the food web was not the main factor explaining the observed spatial TP variation.

A second explanation relates to tuna diet, with tuna from southern regions (ARCHm, SPSGm) relying on a diet of higher TP compared to northern regions (WARMm, PEQD). The results from our study showed that tuna TP estimates were explained more by environmental variables directly constraining tuna vertical habitat (i.e., depth of the 20°C isotherm) for bigeye and yellowfin tuna rather than by surface environmental variables (i.e., NPP and SST) or biological variables (FL). The depth of the 20°C isotherm is a commonly used proxy for the thermocline waters (Fuller et al., 2015), and is used here as such to represent the potential vertical habitat of tuna, with a deeper thermocline leading to a larger vertical habitat. We then hypothesize that this increased vertical habitat in the southern regions would allow tuna greater access to mesopelagic micronekton prey of higher TP. Temperature and oxygen are indeed known to restrict vertical distribution of tuna (Brill, 1994; Graham and Dickson, 2004). Strong spatial trends in the vertical structure of temperature exist in the Western and Central Pacific Ocean, with the depth of the 20°C isotherm ranging from ~140 m in the western equatorial Pacific (WARMm) to ~240 m along 20°S (ARCHm and SPSGm; Fig. 6). The vertical structure of oxygen also displays latitudinal and longitudinal trends with the depth of the 160  $\mu\text{M}$   $\text{O}_2$  (d160) being at ~1200 m in ARCHm, ~350 m in SPSGm and ~200 m along the equator (WARMm). These spatial variations in temperature and oxygen potentially impact the vertical distribution of tuna.

Variations in vertical foraging habitat have been shown to explain intra-specific dietary differences at small spatial scales (Potier et al., 2004; Olson et al., 2010; Williams et al., 2015). For example, the vertical behavior and diet of albacore tuna differed substantially between tropical and temperate latitudes in the South Pacific Ocean, and this was related to the thermal structure of oceanic waters (Williams et al., 2015). Similarly, Olson et al. (2010) observed a higher TP for yellowfin tuna offshore compared to inshore waters in the Eastern Pacific Ocean and related it to offshore access to a higher volume of habitat and to prey of higher TPs.

Tagging data from 4 bigeye tuna in our study revealed that the average seawater temperature the 4 individuals were exposed to over 24 h was close to 20°C, giving further support to the use of the depth of the 20°C isotherm as a proxy for the vertical habitat of tuna. The depth of the 20°C isotherm was positively correlated with TP estimates of bigeye and to a lesser extent of yellowfin, with higher TP estimates with increasing the depth of the 20°C isotherm. Yellowfin tuna mainly inhabit shallow and warm waters above 150 m and feed on epipelagic prey and to a lesser extent on mesopelagic prey compared to bigeye, which forage deeper in the water column on mesopelagic prey (Josse et al., 1998; Brill et al., 1999; Weng et al., 2009; Young et al., 2010). Thus, yellowfin mostly inhabiting seawaters shallower than 150 m might not benefit as much as bigeye from the deepening of the depth of the 20°C isotherm to 240 m at 20°S (Fig. 8). For bigeye, a deeper habitat in the southern regions (ARCHm) was supported by archival tag data, where the mean diving depth of bigeye was higher in New Caledonia than in the western equatorial Pacific (WARMm, depth difference of 50–90 m according to individuals). This shift in bigeye vertical habitat coincides with the spatial distribution of the depth of the 20°C isotherm that is on average located ~50 m deeper in the southern regions (ARCHm) compared to the equatorial zones (WARMm). A deeper 20°C isotherm in ARCHm may allow bigeye tuna to access greater depths and prey of higher TP (Fig. 8).

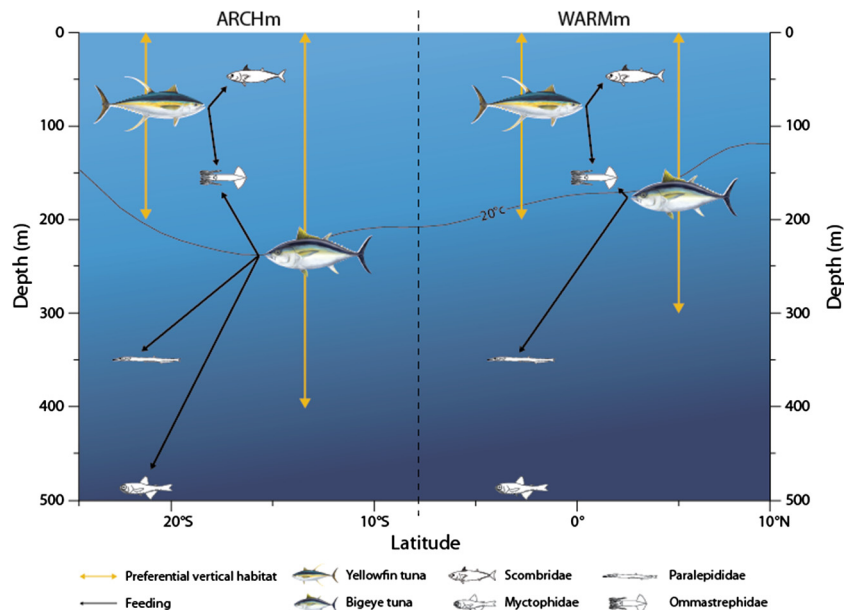


**Fig. 8.** Conceptual diagram of preferential vertical habitat and feeding of yellowfin and bigeye tuna in the two contrasted biochemical regions defined in our study, Archipelagic Deep Basins modified (ARCHm) and Warm Pool modified (WARMm).

Average depths found in this study are based on a small number of tagging individuals. However Fuller et al. (2015) found similar ranges of average daytime depth ( $\sim 330$  m) from a large number of tagged bigeye tuna in the equatorial zone (WARMm) and Evans et al. (2008) reported bigeye tuna of comparable size in the western Pacific Ocean (ARCHm) to have deeper daytime depths at about 400–450 m, which reinforce the idea of a deepening of bigeye vertical habitat in the southern regions. Fuller et al. (2015) also suggested a positive relationship between the deepening of the thermocline and average bigeye daytime depths from west to east in the equatorial Pacific region. Thermocline depth cannot be considered as the depth of feeding but we hypothesize that a deeper vertical habitat could give access to a greater diversity of prey with higher TP.

Giving further support to this vertical habitat hypothesis and, in turn to an access to different prey communities at greater depth, a recent stomach content analysis study revealed spatial difference in the prey composition and diet diversity of bigeye tuna within the Western and Central Pacific Ocean (Duffy et al., in press). Specifically, the authors found a diet shift at 14°S with bigeye exhibiting an increase in the consumption of deeper preys south of 14°S (mesopelagic species > 500 m such as some Myctophidae). Our understanding of micronekton diet of top pelagic predators is scarce but several studies suggested that deeper micronekton species could be more carnivorous and have higher TP's than upper mesopelagic and epipelagic species. Indeed, Burghart et al. (2010) found that the diets of bathypelagic species were largely carnivorous with a higher proportion of fish consumption than their mesopelagic counterparts. Furthermore, using AA-CSIA, Hannides et al. (2013) found that zooplankton TP increased by up to 0.65 between the surface ocean and the mesopelagic zone providing evidence for changes in food resources between epipelagic and mesopelagic zooplankton communities. Indeed, feeding on sinking particles had been shown to be insufficient to respond to mesopelagic zooplankton metabolism (Steinberg et al., 2008; Wilson et al., 2008). Instead, difference in zooplankton TP at depth was more likely driven by a carnivorous feeding on other zooplankton species performing diel vertical migration (Hannides et al., 2013). This difference in TP in the mesopelagic zone could then be transferred

to consumers that access this resource. In addition, Choy et al. (2012) found differences in TP among mesopelagic micronekton species with dragonfishes (family Stomiidae) having higher TP estimates than lanternfishes (family Myctophidae). It is however not clear that these differences are related to depth as these two families seem to have a similar depth repartition (Choy et al., 2012). More AA-CSIA on non-migrant micronekton species, such as Paralepididae and Sternoptychidae (200–500 m), or Chiasmodontidae (>500 m), is required to confirm that higher TP for tuna foraging deeper in the southern regions would be due to foraging on prey of higher TP due to a larger proportion of carnivorous diet for micronekton species occurring therein. Mercury isotope analysis could also assist to track meso-pelagic feeding of tuna as Blum et al. (2013) showed that mercury isotope signatures of pelagic fishes were correlated to their foraging depth.

Combining AA-CSIA and bulk  $\delta^{15}\text{N}$  analysis allowed us to overcome some limitations from baseline effects when assessing predator TP over large spatial scales. Our goal was not to assess the performance of either techniques in producing TP estimates, but rather to verify they resulted in coherent spatial trends in tuna TP. However, we should note that TP estimates based on bulk analyses present some limitations due to TEF and POM assessment. First, while mean tuna TP estimates based on bulk analyses by region gave relatively coherent values when compared with AA-CSIA and the literature (TP estimates between 3.6 and 5.6), individual outliers were found with values as high as 8 and as low as 2 (less than 6% of the data, see Fig. 6). These unrealistic values can be attributed to isotope mismatch between POM and tuna  $\delta^{15}\text{N}$  values, e.g.: migrating tunas that display different bulk  $\delta^{15}\text{N}$  values compared to the average value at the capture location and/or to a potentially inaccurate assessment of POM  $\delta^{15}\text{N}$  values. For example, POM  $\delta^{15}\text{N}$  values have been shown to increase with depth due to preferential bacterial degradation of depleted  $^{15}\text{N}$  organic matter (Saino and Hattori, 1987; Altabet, 1988; Hannides et al., 2013). By accessing greater depths, tuna can forage on mesopelagic prey that relies on a  $^{15}\text{N}$  enriched, sinking POM baseline. Therefore our use of surface POM as the baseline may have overestimated tuna TP. Additionally, the turnover rates of nitrogen isotopes in POM is higher (weeks; Rolff, 2000; Dore et al., 2002) compared

to the tissue of long live top predators (several months; Madigan et al., 2012). Those differences in response times, in addition with potential tuna migration, can thus introduce a bias when estimating tuna TP over large spatial scales (O'Reilly et al., 2002; Richert et al., 2015). In order to constrain isotopic mismatch linked to POM data, Post (2002) suggested using primary consumers as baseline, but over our large spatial scale, this data was not available. Using a different TEF, such as 3.4 (Minagawa and Wada, 1984; Post, 2002), would modify the absolute TP estimates developed in this study, but not the spatial patterns observed. Caut et al. (2009) suggested applying different TEF depending on the baseline  $\delta^{15}\text{N}$  value, which would modify or reduce our TP spatial variations. However their results remain controversial (see Perga and Grey, 2010) as there is no functional explanation for higher TEF in regions of low  $\delta^{15}\text{N}$  values. A different TEF could be pertinent if tuna had access to food with low protein content in a low baseline region as several studies have now demonstrated higher TEF when low quality food was provided to consumers (Vanderklift and Ponsard, 2003). This would however be highly hypothetical in our study, and, given that AA-CSIA confirmed at least partially the TP latitudinal patterns, we are confident of our interpretation of these spatial variations.

In conclusion, correcting for baseline through bulk stable isotope POM-based isoscape for the Western and Central Pacific Ocean and data from AA-CSIA enables this study to overcome some of the limitations in the interpretation of the spatial variations observed in tuna. In the absence of large scale AA data, our study showed that bulk  $\delta^{15}\text{N}$  analyses can be used to provide reasonable mean estimates of TP at large spatial scales (even if this is not true at an individual scale). Combining stable isotope techniques and archival tagging data suggest that bigeye TP (and to a lesser extent yellowfin TP) is influenced by its vertical habitat, which depends on the thermal structure of pelagic habitat (depth of the 20°C isotherm). Our study indicate that thermocline depth might be an important factor to consider in trophic studies and more AA-CSIA data on several tuna species are now needed to investigate further this spatial pattern on other tropical tuna. With the current and projected warming of the upper ocean (e.g., Bopp et al., 2013), tropical tuna could occupy deeper habitats, leading to higher tuna TP estimates in the Western and Central Pacific Ocean altering energy pathways and the function and structure of marine pelagic food webs.

## Acknowledgments

We are grateful to a large team of observers and supervisors from the National Observer Programs of the Pacific Island Countries and Territories and FSM Arrangement Observer Program who collected the tuna samples in the western and central Pacific Ocean. We would like to thank the WCPFC (Western and Central Pacific Fisheries Commission) and the SPC tissue banks which gave us access to the tuna samples. Funding was provided from the GOPS HISPANIC and PACIMER projects, the Pacific Fund VACOPA project, the Government of New Caledonia and NIWA. PH had a fellowship from the Government of New Caledonia, AR from the BIOPELAGOS project funded by the European Union BEST 2.0 Programme and LC was supported by the "Laboratoire d'Excellence" LabexMER (ANR-10-LABX-19). We thank Takuhei Shiozaki and Christine Dupuy who provided POM  $\delta^{15}\text{N}$  values, Thomas Max work on the amino acid compound-specific isotope analysis, Gaël Guillou for stable isotope analysis and Boris Colas from SPC for producing Fig. 8. We thank the University of Tokyo, JAMSTEC and the crew of NO Alis, Hakuho Maru and Atalante for the different cruises that allowed POM sampling: Cassiopee, MoorSpice, Nectalis 3 and 4, Outpace, Pandora and KH13. This work is a contribution to GLOBEC-CLIoTOP WG3/Task Team 2016-01.

## Appendix A. Supplementary material

Supplementary data associated with this article can be found, in the online version, at <http://dx.doi.org/10.1016/j.pocean.2017.04.008>.

## References

- Altabet, M.A., 2006. Isotopic tracers of the marine nitrogen cycle: present and past. In: Volkman, J.K. (Ed.), *Marine Organic Matter: Biomarkers, Isotopes and DNA*. Springer-Verlag, Berlin/Heidelberg, pp. 251–293.
- Altabet, M.A., 2001. Nitrogen isotopic evidence for micronutrient control of fractional NO utilization in the Limnol. Oceanogr. 46, 368–380.
- Altabet, M.A., 1988. Variations in nitrogen isotopic composition between sinking and suspended particles: implications for nitrogen cycling and particle transformation in the open ocean. Deep Sea Res. A: Oceanogr. Res. Pap. 35, 535–554. [http://dx.doi.org/10.1016/0198-0149\(88\)90130-6](http://dx.doi.org/10.1016/0198-0149(88)90130-6).
- Baird, M.E., Timko, P.G., Middleton, J.H., Mullaney, T.J., Cox, D.R., Suthers, I.M., 2008. Biological properties across the Tasman Front off southeast Australia. Deep Sea Res. Oceanogr. Res. Pap. 55, 1438–1455. <http://dx.doi.org/10.1016/j.dsr.2008.06.011>.
- Baum, J.K., Worm, B., 2009. Cascading top-down effects of changing oceanic predator abundances. J. Anim. Ecol. 78, 699–714. <http://dx.doi.org/10.1111/j.1365-2656.2009.01531.x>.
- Behrenfeld, M.J., Falkowski, P.G., 1997. Photosynthetic rates derived from satellite-based chlorophyll concentration. Limnol. Oceanogr. 42, 1–20.
- Bell, J.D., Allain, V., Allison, E.H., Andréfouët, S., Andrew, N.L., Batty, M.J., Blanc, M., Dambacher, J.M., Hampton, J., Hanich, Q., Harley, S., Lorrain, A., McCoy, M., McTurk, N., Nicol, S., Pilling, G., Point, D., Sharp, M.K., Vivili, P., Williams, P., 2015. Diversifying the use of tuna to improve food security and public health in Pacific Island countries and territories. Mar. Policy 51, 584–591. <http://dx.doi.org/10.1016/j.marpol.2014.10.005>.
- Blum, J.D., Popp, B.N., Drazen, J.C., Anela Choy, C., Johnson, M.W., 2013. Methylmercury production below the mixed layer in the North Pacific Ocean. Nat. Geosci. 6, 879–884. <http://dx.doi.org/10.1038/ngeo1918>.
- Bonnet, S., Biegala, I.C., Dutrieux, P., Slemmons, L.O., Capone, D.G., 2009. Nitrogen fixation in the western equatorial Pacific: rates, diazotrophic cyanobacterial size class distribution, and biogeochemical significance. Glob. Biogeochem. Cycles 23. <http://dx.doi.org/10.1029/2008GB003439>.
- Bopp, L., Resplandy, L., Orr, J.C., Doney, S.C., Dunne, J.P., Gehlen, M., Halloran, P., Heinze, C., Ilyina, T., Séférian, R., Tjiputra, J., Vichi, M., 2013. Multiple stressors of ocean ecosystems in the 21st century: projections with CMIP5 models. Biogeosciences 10, 6225–6245. <http://dx.doi.org/10.5194/bg-10-6225-2013>.
- Bradley, C.J., Madigan, D.J., Block, B.A., Popp, B.N., 2014. Amino acid isotope incorporation and enrichment factors in Pacific Bluefin Tuna, *Thunnus orientalis*. PLoS ONE 9, e85818. <http://dx.doi.org/10.1371/journal.pone.0085818>.
- Brill, R.W., 1994. A review of temperature and oxygen tolerance studies of tunas pertinent to fisheries oceanography, movement models and stock assessments. Fish. Oceanogr. 3, 204–216.
- Brill, R.W., Bigelow, K.A., Musyl, M.K., Fritsches, K.A., Warrant, E.J., 2005. Bigeye tuna (*Thunnus obesus*) behavior and physiology and their relevance to stock assessments and fishery biology. Col. Vol. Sci. Pap. ICCAT 57, 142–161.
- Brill, R.W., Block, B.A., Boggs, C.H., Bigelow, K.A., Freund, E.V., Marcinek, D.J., 1999. Horizontal movements and depth distribution of large adult yellowfin tuna (*Thunnus albacares*) near the Hawaiian Islands, recorded using ultrasonic telemetry: implications for the physiological ecology of pelagic fishes. Mar. Biol. 133, 395–408.
- Burghart, S., Hopkins, T., Torres, J., 2010. Partitioning of food resources in bathypelagic micronekton in the eastern Gulf of Mexico. Mar. Ecol. Prog. Ser. 399, 131–140. <http://dx.doi.org/10.3354/meps08365>.
- Campbell, L., Carpenter, E.J., Montoya, J.P., Kustka, A.B., Capone, D.G., 2005. Picoplankton community structure within and outside a Trichodesmium bloom in the southwestern Pacific Ocean. Vie Milieu 55, 185–195.
- Castella, E., Adalsteinsson, H., Brittain, J.E., Gislason, G.M., Lehmann, A., Lencioni, V., Lods-Crozet, B., Maiolini, B., Milner, A.M., Olafsson, J.S., et al., 2001. Macrobenthic invertebrate richness and composition along a latitudinal gradient of European glacier-fed streams. Freshw. Biol. 46, 1811–1831.
- Caut, S., Angulo, E., Courchamp, F., 2009. Variation in discrimination factors ( $\Delta^{15}\text{N}$  and  $\Delta^{13}\text{C}$ ): the effect of diet isotopic values and applications for diet reconstruction. J. Appl. Ecol. 46, 443–453. <http://dx.doi.org/10.1111/j.1365-2664.2009.01620.x>.
- Choy, C.A., Davison, P.C., Drazen, J.C., Flynn, A., Gier, E.J., Hoffman, J.C., McClain-Counts, J.P., Miller, T.W., Popp, B.N., Ross, S.W., Sutton, T.T., 2012. Global trophic position comparison of two dominant mesopelagic fish families (Mycetophidae, Stomiidae) using amino acid nitrogen isotopic analyses. PLoS ONE 7, e50133. <http://dx.doi.org/10.1371/journal.pone.0050133>.
- Choy, C.A., Popp, B.N., Hannides, C.C.S., Drazen, J.C., 2015. Trophic structure and food resources of epipelagic and mesopelagic fishes in the North Pacific Subtropical Gyre ecosystem inferred from nitrogen isotopic compositions: trophic structure of pelagic fishes. Limnol. Oceanogr. 60, 1156–1171. <http://dx.doi.org/10.1002/lno.10085>.
- Deutsch, C., Gruber, N., Key, R.M., Sarmiento, J.L., 2001. Denitrification and N<sub>2</sub> fixation in the Pacific Ocean. Glob. Biogeochem. Cycles 15, 483–506. <http://dx.doi.org/10.1029/2000GB001291>.

- Dore, J.E., Brum, J.R., Tupas, L.M., Karl, D.M., 2002. Seasonal and interannual variability in sources of nitrogen supporting export in the oligotrophic subtropical North Pacific Ocean. *Limnol. Oceanogr.* 47, 1595–1607.
- Duffy, L.M., Kuhnert, P., Pethybridge, H.R., Young, J.W., Olson, R.J., Logan, J.M., Goñi, N., Romanov, E., Allain, V., Staudinger, M., Abecassis, M., Choy, C.A., Hobday, A.J., Simier, M., Galván-Magaña, F., Potier, M., Ménard, F., 2017. Global trophic ecology of yellowfin, bigeye and albacore tunas: understanding tuna predation on micronekton communities at ocean-basin scales. *Deep Sea Res. II Top. Stud. Oceanogr.* (in press), <http://dx.doi.org/10.1016/j.dsr2.2017.03.003>.
- Estes, J.A., Terborgh, J., Brashares, J.S., Power, M.E., Berger, J., Bond, W.J., Carpenter, S.R., Essington, T.E., Holt, R.D., Jackson, J.B.C., Marquis, R.J., Oksanen, L., Oksanen, T., Paine, R.T., Pickett, E.K., Ripple, W.J., Sandin, S.A., Scheffer, M., Schoener, T.W., Shurin, J.B., Sinclair, A.R.E., Soule, H.E., Virtanen, R., Wardle, D.A., 2011. Trophic downgrading of planet Earth. *Science* 333, 301–306. <http://dx.doi.org/10.1126/science.1205106>.
- Evans, K., Langley, A., Clear, N.P., Williams, P., Patterson, T., Sibert, J., Hampton, J., Gunn, J.S., 2008. Behaviour and habitat preferences of bigeye tuna (*Thunnus obesus*) and their influence on longline fishery catches in the western Coral Sea. *Can. J. Fish. Aquat. Sci.* 65, 2427–2443. <http://dx.doi.org/10.1139/F08-148>.
- Fonteneau, A., Hallier, J.P., 2015. Fifty years of dart tag recoveries for tropical tuna: a global comparison of results for the western Pacific, eastern Pacific, Atlantic, and Indian Oceans. *Fish. Res.* 163, 7–22. <http://dx.doi.org/10.1016/j.fishres.2014.03.022>.
- Fry, B., 2006. *Stable Isotope Ecology*. Springer, New York, NY.
- Fuller, D.W., Schaefer, K.M., Hampton, J., Caillot, S., Leroy, B.M., Itano, D.G., 2015. Vertical movements, behavior, and habitat of bigeye tuna (*Thunnus obesus*) in the equatorial central Pacific Ocean. *Fish. Res.* 172, 57–70. <http://dx.doi.org/10.1016/j.fishres.2015.06.024>.
- Gallardo, B., Gascón, S., González-Sanchís, M., Cabezas, A., Comín, F.A., 2009. Modelling the response of floodplain aquatic assemblages across the lateral hydrological connectivity gradient. *Mar. Freshw. Res.* 60, 924. <http://dx.doi.org/10.1071/MF08277>.
- Ganachaud, A., Sen Gupta, A., Brown, J.N., Evans, K., Maes, C., Muir, L.C., Graham, F.S., 2013. Projected changes in the tropical Pacific Ocean of importance to tuna fisheries. *Clim. Change* 119, 163–179. <http://dx.doi.org/10.1007/s10584-012-0631-1>.
- García, H.E., Locarnini, R.A., Boyer, T.P., Antonov, J.I., Mishonov, A.V., Baranova, O.K., Zweng, M.M., Reagan, J.R., Johnson, D.R., 2013. *World Ocean Atlas 2013*. In: Levitus, S., Mishonov, A.V. (Eds.), *Dissolved Oxygen, Apparent Oxygen Utilization, and Oxygen Saturation*, vol. 3. NOAA Atlas NESDIS, p. 27.
- Gaston, T.F., Suthers, I.M., 2004. Spatial variation in  $\delta^{13}\text{C}$  and  $\delta^{15}\text{N}$  of liver, muscle and bone in a rocky reef planktivorous fish: the relative contribution of sewage. *J. Exp. Mar. Biol. Ecol.* 304, 17–33. <http://dx.doi.org/10.1016/j.jembe.2003.11.022>.
- Graham, B.S., Koch, P.L., Newsome, S.D., McMahon, K.W., Aurioles, D., 2010. Using isotopes to trace the movements and foraging behavior of top predators in oceanic ecosystems. In: West, J.B., Bowen, G.J., Dawson, T.E., Tu, K.P. (Eds.), *Isoscapes*. Springer, Netherlands, Dordrecht, pp. 299–318.
- Graham, J.B., Dickson, K.A., 2004. Tuna comparative physiology. *J. Exp. Biol.* 207, 4015–4024. <http://dx.doi.org/10.1242/jeb.01267>.
- Gunn, J., Block, B.A., 2001. Advances in acoustic, archival, and satellite tagging of tunas. In: Block, B.A., Stevens, D.E. (Eds.), *Tuna: Physiology, Ecology and Evolution*. Academic Press, San Diego, California, pp. 167–224.
- Gutiérrez-Rodríguez, A., Décima, M., Popp, B.N., Landry, M.R., 2014. Isotopic invisibility of protozoan trophic steps in marine food webs. *Limnol. Oceanogr.* 59, 1590–1598. <http://dx.doi.org/10.4319/lo.2014.59.5.1590>.
- Hampton, J., Gunn, J., 1998. Exploitation and movements of yellowfin tuna (*Thunnus albacares*) and bigeye tuna (*T. obesus*) tagged in the north-western Coral Sea. *Mar. Freshw. Res.* 49, 475–489.
- Hannides, C.C., Popp, B.N., Landry, M.R., Graham, B.S., 2009. Quantification of zooplankton trophic position in the North Pacific Subtropical Gyre using stable nitrogen isotopes. *Limnol. Oceanogr.* 54, 50.
- Hannides, C.C.S., Popp, B.N., Choy, C.A., Drazen, J.C., 2013. Midwater zooplankton and suspended particle dynamics in the North Pacific Subtropical Gyre: a stable isotope perspective. *Limnol. Oceanogr.* 58, 1931–1946. <http://dx.doi.org/10.4319/lo.2013.58.6.1931>.
- Hastie, T.J., Tibshirani, R.J., 1990. *Generalized Additive Models, Monographs on Statistics and Applied Probability*. Chapman and Hall/CRC, London.
- Hayes, J.M., Freeman, K.H., Popp, B.N., Hoham, C.H., 1990. Compound-specific isotopic analyses: a novel tool for reconstruction of ancient biogeochemical processes. *Org. Geochem.* 16, 1115–1128.
- Hays, G., Richardson, A., Robinson, C., 2005. Climate change and marine plankton. *Trends Ecol. Evol.* 20, 337–344. <http://dx.doi.org/10.1016/j.tree.2005.03.004>.
- Hetherington, E.D., Olson, R.J., Drazen, J.C., Lennert-Cody, C.E., Ballance, L.T., Kaufmann, R.S., Popp, B.N., 2016. Spatial food-web structure in the eastern tropical Pacific Ocean based on compound-specific nitrogen isotope analysis of amino acids: food web structure based on  $\delta^{15}\text{N}$ . *Limnol. Oceanogr.* <http://dx.doi.org/10.1002/lno.10443>.
- Hobday, A.J., Arrizabalaga, H., Evans, K., Nicol, S., Young, J.W., Weng, K.C., 2015. Impacts of climate change on marine top predators: advances and future challenges. *Deep Sea Res. II Top. Stud. Oceanogr.* 113, 1–8. <http://dx.doi.org/10.1016/j.dsr2.2015.01.013>.
- Hunt, B.P.V., Allain, V., Menkes, C.E., Lorrain, A., Graham, B., Rodier, M., Pagano, M., Carlotti, F., 2015. A coupled stable isotope-size spectrum approach to understanding pelagic food-web dynamics: a case study from the southwest sub-tropical Pacific. *Deep Sea Res. II Top. Stud. Oceanogr.* 113, 208–224. <http://dx.doi.org/10.1016/j.dsr2.2014.10.023>.
- Josse, E., Bach, P., Dagorn, L., 1998. Simultaneous observations of tuna movements and their prey by sonic tracking and acoustic surveys. *Hydrobiologia* 371, 61–69. <http://dx.doi.org/10.1023/A:1017065709190>.
- Lam, C.H., Galuardi, B., Lutcavage, M.E., 2014. Movements and oceanographic associations of bigeye tuna (*Thunnus obesus*) in the Northwest Atlantic. *Can. J. Fish. Aquat. Sci.* 71, 1529–1543. <http://dx.doi.org/10.1139/cjfas-2013-0511>.
- Le Borgne, R., Allain, V., Griffiths, S.P., Matear, R.J., McKinnon, A.D., Richardson, A.J., Young, J.W., 2011. Chapter 4, Vulnerability of open ocean food webs in the tropical Pacific to climate change. In: Bell, J.D., Hobday, A.J. (Eds.), *Vulnerability of Tropical Pacific Fisheries and Aquaculture to Climate Change*. Secretariat of the Pacific Community, New Caledonia, pp. 189–249.
- Leroy, B., Phillips, J.S., Nicol, S., Pilling, G.M., Harley, S., Bromhead, D., Hoyle, S., Caillot, S., Allain, V., Hampton, J., 2013. A critique of the ecosystem impacts of drifting and anchored FADs use by purse-seine tuna fisheries in the Western and Central Pacific Ocean. *Aquat. Living Resour.* 26, 49–61. <http://dx.doi.org/10.1051/alr/2012033>.
- Longhurst, A.R., 2007. *Ecological Geography of the Sea*. Academic Press, Amsterdam, Boston, MA.
- Lorrain, A., Graham, B.S., Popp, B.N., Allain, V., Olson, R.J., Hunt, B.P.V., Potier, M., Fry, B., Galván-Magaña, F., Menkes, C.E.R., Kaehler, S., Ménard, F., 2015. Nitrogen isotopic baselines and implications for estimating foraging habitat and trophic position of yellowfin tuna in the Indian and Pacific Oceans. *Deep Sea Res. II Top. Stud. Oceanogr.* 113, 188–198. <http://dx.doi.org/10.1016/j.dsr2.2014.02.003>.
- Madigan, D.J., Litvin, S.Y., Popp, B.N., Carlisle, A.B., Farwell, C.J., Block, B.A., 2012. Tissue turnover rates and isotopic trophic discrimination factors in the endothermic teleost, Pacific Bluefin Tuna (*Thunnus orientalis*). *PLoS ONE* 7, e49220. <http://dx.doi.org/10.1371/journal.pone.0049220>.
- Marasco, R.J., Goodman, D., Grimes, C.B., Lawson, P.W., Punt, A.E., Quinn II, T.J., 2007. Ecosystem-based fisheries management: some practical suggestions. *Can. J. Fish. Aquat. Sci.* 64, 928–939.
- McClelland, J.W., Montoya, J.P., 2002. Trophic relationships and the nitrogen isotopic composition of amino acids in plankton. *Ecology* 83, 2173–2180.
- McMahon, K.W., Hamady, L.L., Thorold, S.R., 2013. Ocean ecogeochemistry: a review. *Oceanogr. Mar. Biol. Annu. Rev.* 51, 327–374.
- Ménard, F., Lorrain, A., Potier, M., Marsac, F., 2007. Isotopic evidence of distinct feeding ecologies and movement patterns in two migratory predators (yellowfin tuna and swordfish) of the western Indian Ocean. *Mar. Biol.* 153, 141–152. <http://dx.doi.org/10.1007/s00227-007-0789-7>.
- Minagawa, M., Wada, E., 1984. Stepwise enrichment of  $^{15}\text{N}$  along food chains: further evidence and the relation between  $\delta^{15}\text{N}$  and animal age. *Geochim. Cosmochim. Acta* 48, 1135–1140.
- Moisander, P.H., Beinart, R.A., Hewson, I., White, A.E., Johnson, K.S., Carlson, C.A., Montoya, J.P., Zehr, J.P., 2010. Unicellular cyanobacterial distributions broaden the oceanic N<sub>2</sub> fixation domain. *Science* 327, 1512–1514. <http://dx.doi.org/10.1126/science.1185468>.
- Navarro, J., Coll, M., Somes, C.J., Olson, R.J., 2013. Trophic niche of squids: insights from isotopic data in marine systems worldwide. *Deep Sea Res. II Top. Stud. Oceanogr.* 95, 93–102. <http://dx.doi.org/10.1016/j.dsr2.2013.01.031>.
- Nielsen, A., Bigelow, K.A., Musyl, M.K., Sibert, J.R., 2006. Improving light-based geolocation by including sea surface temperature. *Fish. Oceanogr.* 15, 314–325. <http://dx.doi.org/10.1111/j.1365-2419.2005.00401.x>.
- Nielsen, A., Sibert, J.R., 2007. State-space model for light-based tracking of marine animals. *Can. J. Fish. Aquat. Sci.* 64, 1055–1068. <http://dx.doi.org/10.1139/F07-064>.
- Nielsen, J.M., Popp, B.N., Winder, M., 2015. Meta-analysis of amino acid stable nitrogen isotope ratios for estimating trophic position in marine organisms. *Oecologia* 178, 631–642. <http://dx.doi.org/10.1007/s00442-015-3305-7>.
- Olson, R., Duffy, L., Kuhnert, P., Galván-Magaña, F., Bocanegra-Castillo, N., Alatorre-Ramírez, V., 2014. Decadal diet shift in yellowfin tuna *Thunnus albacares* suggests broad-scale food web changes in the eastern tropical Pacific Ocean. *Mar. Ecol. Prog. Ser.* 497, 157–178. <http://dx.doi.org/10.3354/meps10609>.
- Olson, R.J., Popp, B.N., Graham, B.S., López-Ibarra, G.A., Galván-Magaña, F., Lennert-Cody, C.E., Bocanegra-Castillo, N., Wallsgrove, N.J., Gier, E., Alatorre-Ramírez, V., Ballance, L.T., Fry, B., 2010. Food-web inferences of stable isotope spatial patterns in copepods and yellowfin tuna in the pelagic eastern Pacific Ocean. *Prog. Oceanogr.* 86, 124–138. <http://dx.doi.org/10.1016/j.pocan.2010.04.026>.
- O'Reilly, C.M., Hecky, R.E., Cohen, A.S., Plisnier, P.D., 2002. Interpreting stable isotopes in food webs: recognizing the role of time averaging at different trophic levels. *Limnol. Oceanogr.* 47, 306–309.
- Perga, M.E., Grey, J., 2010. Laboratory measures of isotope discrimination factors: comments on Caut, Angulo & Courchamp (2008, 2009): comments on Caut, Angulo & Courchamp (2008). *J. Appl. Ecol.* 47, 942–947. <http://dx.doi.org/10.1111/j.1365-2664.2009.01730.x>.
- Polovina, J.J., Howell, E.A., Abecassis, M., 2008. Ocean's least productive waters are expanding. *Geophys. Res. Lett.* 35, L03618. <http://dx.doi.org/10.1029/2007GL031745>.
- Popp, B.N., Graham, B.S., Olson, R.J., Hannides, C.C., Lott, M.J., López-Ibarra, G.A., Galván-Magaña, F., Fry, B., 2007. Insight into the trophic ecology of yellowfin tuna, *Thunnus albacares*, from compound-specific nitrogen isotope analysis of proteinaceous amino acids. *Terr. Ecol.* 1, 173–190.
- Post, D.M., 2002. Using stable isotopes to estimate trophic position: models, methods, and assumptions. *Ecology* 83, 703. <http://dx.doi.org/10.2307/3071875>.

- Potier, M., Marsac, F., Lucas, V., Sabatié, R., Hallier, J.P., Ménard, F., 2004. Feeding partitioning among tuna taken in surface and mid-water layers: the case of yellowfin (*Thunnus albacares*) and bigeye (*T. obesus*) in the western tropical Indian Ocean. *West. Indian Ocean J. Mar. Sci.* 3, 51–62.
- R Core Team, 2016. R: A Language and Environment for Statistical Computing. R Foundation for Statistical Computing, Vienna, Austria. ISBN: 3-900051-07-0 <<https://www.R-project.org/>>.
- Rafter, P.A., DiFiore, P.J., Sigman, D.M., 2013. Coupled nitrate nitrogen and oxygen isotopes and organic matter remineralization in the Southern and Pacific Oceans: nitrate isotopes and remineralization. *J. Geophys. Res. Oceans* 118, 4781–4794. <http://dx.doi.org/10.1002/jgrc.20316>.
- Rafter, P.A., Sigman, D.M., 2016. Spatial distribution and temporal variation of nitrate nitrogen and oxygen isotopes in the upper equatorial Pacific Ocean: equatorial Pacific nitrate N and O isotopes. *Limnol. Oceanogr.* 61, 14–31. <http://dx.doi.org/10.1002/lno.10152>.
- Raimbault, P., García, N., Cerutti, F., 2008. Distribution of inorganic and organic nutrients in the South Pacific Ocean—evidence for long-term accumulation of organic matter in nitrogen-depleted waters. *Biogeosciences* 5, 281–298.
- Reynolds, R.W., Rayner, N.A., Smith, T.M., Stokes, D.C., Wang, W., 2002. An improved in situ and satellite SST analysis for climate. *J. Clim.* 15, 1609–1625.
- Richert, J.E., Galván-Magaña, F., Klimley, A.P., 2015. Interpreting nitrogen stable isotopes in the study of migratory fishes in marine ecosystems. *Mar. Biol.* 162, 1099–1110. <http://dx.doi.org/10.1007/s00227-015-2652-6>.
- Rolff, C., 2000. Seasonal variation in  $\delta^{13}\text{C}$  and  $\delta^{15}\text{N}$  of size-fractionated plankton at a coastal station in the northern Baltic proper. *Mar. Ecol. Prog. Ser.* 203, 47–65.
- Saino, T., Hattori, A., 1987. Geographical variation of the water column distribution of suspended particulate organic nitrogen and its  $^{15}\text{N}$  natural abundance in the Pacific and its marginal seas. *Deep Sea Res. A: Oceanogr. Res. Pap.* 34, 807–827. [http://dx.doi.org/10.1016/0198-0149\(87\)90038-0](http://dx.doi.org/10.1016/0198-0149(87)90038-0).
- Schaefer, K., Fuller, D., Hampton, J., Caillot, S., Leroy, B., Itano, D., 2015. Movements, dispersion, and mixing of bigeye tuna (*Thunnus obesus*) tagged and released in the equatorial Central Pacific Ocean, with conventional and archival tags. *Fish. Res.* 161, 336–355. <http://dx.doi.org/10.1016/j.fishres.2014.08.018>.
- Schaefer, K.M., Fuller, D.W., 2010. Vertical movements, behavior, and habitat of bigeye tuna (*Thunnus obesus*) in the equatorial eastern Pacific Ocean, ascertained from archival tag data. *Mar. Biol.* 157, 2625–2642. <http://dx.doi.org/10.1007/s00227-010-1524-3>.
- Schaefer, K.M., Fuller, D.W., 2002. Movements, behavior, and habitat selection of bigeye tuna (*Thunnus obesus*) in the eastern equatorial Pacific, ascertained through archival tags. *Fish. Bull.* 100, 765–788.
- Schaefer, K.M., Fuller, D.W., Block, B.A., 2009. Vertical movements and habitat utilization of skipjack (*Katsuwonus pelamis*), yellowfin (*Thunnus albacares*), and bigeye (*Thunnus obesus*) tunas in the equatorial eastern Pacific Ocean, ascertained through archival tag data. In: Nielsen, J.L., Arrizabalaga, H., Fragoso, N., Hobday, A.J., Lutcavage, M.E., Sibert, J.R. (Eds.), *Tagging and Tracking of Marine Animals with Electronic Devices, Reviews: Methods and Technologies in Fish Biology and Fisheries*. Springer, Netherlands, Dordrecht, pp. 121–144.
- Shiozaki, T., Kodama, T., Furuya, K., 2014. Large-scale impact of the island mass effect through nitrogen fixation in the western South Pacific Ocean. *Geophys. Res. Lett.* 41, 2907–2913. <http://dx.doi.org/10.1002/2014GL059835>.
- Sibert, J., Hampton, J., 2003. Mobility of tropical tunas and the implications for fisheries management. *Mar. Policy* 27, 87–95.
- Sigman, D.M., Karsh, K.L., Casciotti, K.L., 2009. Ocean process tracers: nitrogen isotopes in the ocean. *Encycl. Ocean Sci.* 4138–4153.
- Somes, C.J., Schmittner, A., Galbraith, E.D., Lehmann, M.F., Altabet, M.A., Montoya, J. P., Letelier, R.M., Mix, A.C., Bourbonnais, A., Eby, M., 2010. Simulating the global distribution of nitrogen isotopes in the ocean. *Glob. Biogeochem. Cycles* 24, GB4019. <http://dx.doi.org/10.1029/2009GB003767>.
- Sommer, U., Stibor, H., Katschik, A., Sommer, F., Hansen, T., 2002. Pelagic food web configurations at different levels of nutrient richness and their implications for the ratio fish production: primary production. In: Vadstein, O., Olsen, Y. (Eds.), *Sustainable Increase of Marine Harvesting: Fundamental Mechanisms and New Concepts*. Springer, pp. 11–20.
- Steinberg, D.K., Mooy, B.A.V., Buesseler, K.O., Boyd, P.W., Kobari, T., Karl, D.M., 2008. Bacterial vs. zooplankton control of sinking particle flux in the ocean's twilight zone. *Limnol. Oceanogr.* 53, 1327.
- Vanderklift, M.A., Ponsard, S., 2003. Sources of variation in consumer-diet  $\delta^{15}\text{N}$  enrichment: a meta-analysis. *Oecologia* 136, 169–182. <http://dx.doi.org/10.1007/s00442-003-1270-z>.
- Weng, K.C., Stokesbury, M.J.W., Boustany, A.M., Seitz, A.C., Teo, S.L.H., Miller, S.K., Block, B.A., 2009. Habitat and behaviour of yellowfin tuna *Thunnus albacares* in the Gulf of Mexico determined using pop-up satellite archival tags. *J. Fish Biol.* 74, 1434–1449. <http://dx.doi.org/10.1111/j.1095-8649.2009.02209.x>.
- Williams, A.J., Allain, V., Nicol, S.J., Evans, K.J., Hoyle, S.D., Dupoux, C., Vourey, E., Dubosc, J., 2015. Vertical behavior and diet of albacore tuna (*Thunnus alalunga*) vary with latitude in the South Pacific Ocean. *Deep Sea Res. II Top. Stud. Oceanogr.* 113, 154–169. <http://dx.doi.org/10.1016/j.dsr2.2014.03.010>.
- Wilson, S.E., Steinberg, D.K., Buesseler, K.O., 2008. Changes in fecal pellet characteristics with depth as indicators of zooplankton repackaging of particles in the mesopelagic zone of the subtropical and subarctic North Pacific Ocean. *Deep Sea Res. II Top. Stud. Oceanogr.* 55, 1636–1647. <http://dx.doi.org/10.1016/j.dsr2.2008.04.019>.
- Wood, S., 2006. *Generalized Additive Models: An Introduction with R*. CRC Press.
- Yoshikawa, C., Makabe, A., Shiozaki, T., Toyoda, S., Yoshida, O., Furuya, K., Yoshida, N., 2015. Nitrogen isotope ratios of nitrate and  $\text{N}^*$  anomalies in the subtropical South Pacific. *Geochem. Geophys. Geosystems* 16, 1439–1448. <http://dx.doi.org/10.1002/2014GC005678>.
- Yoshikawa, C., Yamanaka, Y., Nakatsuka, T., 2006. Nitrate-nitrogen isotopic patterns in surface waters of the western and central equatorial Pacific. *J. Oceanogr.* 62, 511–525.
- Young, J.W., Hunt, B.P.V., Cook, T.R., Llopiz, J.K., Hazen, E.L., Pethybridge, H.R., Ceccarelli, D., Lorrain, A., Olson, R.J., Allain, V., Menkes, C.E., Patterson, T., Nicol, S., Lehodey, P., Kloser, R.J., Arrizabalaga, H., Anela Choy, C., 2015. The trophodynamics of marine top predators: current knowledge, recent advances and challenges. *Deep Sea Res. II Top. Stud. Oceanogr.* 113, 170–187. <http://dx.doi.org/10.1016/j.dsr2.2014.05.015>.
- Young, J.W., Lansdell, M.J., Campbell, R.A., Cooper, S.P., Juanes, F., Guest, M.A., 2010. Feeding ecology and niche segregation in oceanic top predators off eastern Australia. *Mar. Biol.* 157, 2347–2368. <http://dx.doi.org/10.1007/s00227-010-1500-y>.